The differentiation and integration of the hippocampal dorsoventral axis are controlled by two nuclear receptor genes

Xiong Yang[1#], Rong Wan[1#], Zhiwen Liu[2,3], Su Feng[2,3], Jiaxin Yang[1], Naihe Jing[2,3*], Ke Tang[1*]

1, Precise Genome Engineering Center, School of Life Sciences, Guangzhou University, Guangzhou, Guangdong 510006, China

2, Guangzhou Laboratory/Bioland Laboratory, Guangzhou, 510005, China

3, CAS Key Laboratory of Regenerative Biology, Guangdong Provincial Key Laboratory of Stem Cell and Regenerative Medicine, Guangdong Institutes of Biomedicine and Health, Chinese Academy of Sciences, Guangzhou 510530, China.

#, Co-first authors

*, Co-corresponding authors

Correspondence: njing@sibcb.ac.cn or ktang.sc@gmail.com.

Abstract

The hippocampus executes crucial functions from declarative memory to adaptive behaviors associated with cognition and emotion. However, the mechanisms of how morphogenesis and functions along the hippocampal dorsoventral axis are differentiated and integrated are still largely unclear. Here, we show that *COUP-TFI* and *-TFII* genes are distinctively expressed in the dorsal and ventral hippocampus, respectively. The loss of *COUP-TFII* results in ectopic CA1/CA3 domains in the ventral hippocampus. The deficiency of *COUP-TFI* leads to the failed specification of dorsal CA1, among which there are place cells. The deletion of both *COUP-TF* genes causes almost agenesis of the hippocampus with abnormalities of trisynaptic circuit and adult neurogenesis. Moreover, *COUP-TFI*/*-TFII* may cooperate to guarantee appropriate morphogenesis and function of the hippocampus by regulating the *Lhx5-Lhx2* axis. Our findings revealed a novel mechanism that *COUP-TFI* and *COUP-TFII* converge to govern the differentiation and integration of distinct characteristics of the hippocampus in mice.

Keywords

Memory; Hippocampus; *COUP-TF* Gene; Place Cell; Trisynaptic Circuit

36 **Introduction**

37 Memory, including declarative and nondeclarative memory, unifies our mental world to
38 ensure the quality of life for people of all ages, from newborns to elderly individuals
39 (Eichenbaum & Cohen, 2014; Kandel, Dudai, & Mayford, 2014). The pioneering studies of
40 Milner and her colleagues revealed that the hippocampus is required for declarative memory
41 but not nondeclarative memory (Penfield & Milner, 1958; Scoville & Milner, 1957). The
42 discovery of activity-dependent long-term potentiation and place cells provides the
43 neurophysiological basis of hippocampal function (Bliss & Lomo, 1973; O'Keefe &
44 Dostrovsky, 1971). The rodent hippocampus can be divided into the dorsal and ventral
45 domains, corresponding to the posterior and anterior hippocampus in humans, respectively.
46 In recent decades, numerous studies have supported the Moser theory that the hippocampus is
47 a heterogeneous structure with distinct characteristics of gene expression, connectivity, and
48 functions along its dorsoventral axis (Bast, 2007; Fanselow & Dong, 2010; Moser & Moser,
49 1998; Strange, Witter, Lein, & Moser, 2014). The dorsal hippocampus, which connects and
50 shares similar gene expression with the neocortex (Fanselow & Dong, 2010), serves the "cold"
51 cognitive function associated with declarative memory and spatial navigation. The ventral
52 hippocampus, which connects and generates similar gene expression with the amygdala and
53 hypothalamus (Cenquizca & Swanson, 2007; Kishi et al., 2000; Pitkanen, Pikkarainen,
54 Nurminen, & Ylinen, 2000), corresponds to the "hot" affective states related to emotion and
55 anxiety (Fanselow & Dong, 2010; Tyng, Amin, Saad, & Malik, 2017). Nonetheless, to date,
56 the molecular and cellular mechanisms by which the morphogenesis, connectivity, and
57 functions along the dorsoventral axis of the hippocampus are differentiated and integrated are
58 largely unknown.

59 The hippocampus, a medial temporal lobe structure in the adult rodent forebrain, originates
60 from the medial pallium (MP) in the medial line of the early dorsal telencephalon. The

61 cortical hem (CH), which is located ventrally to the MP, functions as an organizer for
62 hippocampal development (Hébert & Fishell, 2008; Schuurmans & Guillemot, 2002). It has
63 been demonstrated that both extrinsic signals, such as *Wnts* and *Bmps*, and intrinsic factors,
64 including *Emx1*, *Emx2*, *Lef1*, *Lhx2*, and *Lhx5*, are involved in the regulation of early
65 morphogenesis of the hippocampus. As the earliest *Wnt* gene to be exclusively expressed in
66 the cortical hem, *Wnt3a* is required for the genesis of the hippocampus (S. M. Lee, Tole,
67 Grove, & McMahon, 2000); in addition, *Lef1* is downstream of Wnt signaling, and the
68 hippocampus is completely absent in *Lef1-neo/neo* null mutant mice (Galceran, Miyashita-
69 Lin, Devaney, Rubenstein, & Grosschedl, 2000). Wnt signaling is essential for early
70 development of the hippocampus. *Emx1* and *Emx2* are mouse homologs of *Drosophila empty*
71 *spiracles* (Simeone et al., 1992). Interestingly, the dorsal hippocampus is smaller in an *Emx1*
72 null mutant (Yoshida et al., 1997), while *Emx2* is required for the growth of the hippocampus
73 but not for the specification of hippocampal lineages (Tole, Goudreau, Assimacopoulos, &
74 Grove, 2000). Moreover, *Lhx5*, which encodes a LIM homeobox transcription factor and is
75 specifically expressed in the hippocampal primordium, is necessary for the formation of the
76 hippocampus (Zhao et al., 1999). *Lhx2*, encoding another LIM homeobox transcription factor,
77 is required for the development of both the hippocampus and neocortex (Mangale et al., 2008;
78 Monuki, Porter, & Walsh, 2001; Porter et al., 1997). Intriguingly, deficiency of either *Lhx5* or
79 *Lhx2* results in agenesis of the hippocampus, and more particularly, these genes inhibit each
80 other (Hébert & Fishell, 2008; Mangale et al., 2008; Roy, Gonzalez-Gomez, Pierani, Meyer,
81 & Tole, 2014; Zhao et al., 1999), indicating that the *Lhx5* and *Lhx2* genes may generate an
82 essential regulatory axis to ensure the appropriate hippocampal development. Nevertheless,
83 whether there are other intrinsic genes that participate in the regulation of morphogenesis and
84 function of the hippocampus has not been fully elucidated.

85 *COUP-TF* genes, including *COUP-TFI* (also known as *NR2F1*) and *COUP-TFII* (also
86 known as *NR2F2*), encode two transcription factor proteins belonging to the nuclear receptor
87 superfamily (Yang, Feng, & Tang, 2017). Mutations of *COUP-TFI* are highly related to
88 neurodevelopmental disorders (NDD), such as intellectual disability (ID) and autism
89 spectrum disorders (ASD) (Bertacchi et al., 2020; Bosch et al., 2014; Contesse, Ayrault,
90 Mantegazza, Studer, & Deschaux, 2019), and mutations of the *COUP-TFII* gene are
91 associated with congenital heart defects (CHD) (High et al., 2016). By using animal models,
92 our studies and others have demonstrated that *COUP-TF* genes participate in the regulation
93 of the development of the central nervous system (Zhang et al., 2020). The *COUP-TFI* plays
94 an essential role in the differentiation of cortical excitatory projection neurons and inhibitory
95 interneurons, the development of the dorsal hippocampus, and cortical arealization
96 (Armentano et al., 2007; Bertacchi et al., 2020; Del Pino et al., 2020; J. Feng et al., 2021;
97 Flore et al., 2017; Lodato et al., 2011; C. Zhou et al., 1999; C. Zhou, Tsai, & Tsai, 2001).
98 *COUP-TFII* plays a vital role in the development of the amygdala, hypothalamus, and
99 cerebellum (S. Feng et al., 2017; Kim, Takamoto, Yan, Tsai, & Tsai, 2009; Tang, Rubenstein,
100 Tsai, & Tsai, 2012). Nevertheless, whether and how *COUP-TFI* and/or *COUP-TFII* genes
101 regulate the differentiation and integration of hippocampal morphogenesis, connectivity, and
102 function is still largely unclear.
103 Here, our data show that *COUP-TFI* and *-TFII* genes are differentially expressed along the
104 dorsoventral axis of the postnatal hippocampus. The loss of *COUP-TFII* results in ectopic
105 CA1 and CA3 domains in the ventral hippocampus. In addition, the deficiency of *COUP-TFI*
106 leads to not only dysplasia of the dorsal hippocampus but also failed specification and
107 differentiation of the dorsal CA1 pyramidal neuron lineage. Furthermore, the deletion of both
108 genes in the *RXCre*/+; *COUP-TFI*$^{F/F}$; *COUP-TFII*$^{F/F}$ double mutant mouse causes almost
109 agenesis of the hippocampus, accompanied by compromised specification of the CA1, CA3,

110 and dentate gyrus (DG) domains. The components of the trisynaptic circuit are abnormal in
111 the corresponding single-gene or double-gene mutant model. Moreover, *COUP-TF* genes
112 may cooperate to guarantee the appropriate morphogenesis and function of the hippocampus
113 by regulating the *Lhx5-Lhx2* axis.
114
115 **Results**
116 **Differential expression profiles of *COUP-TFI* and *-TFII* genes along the dorsoventral**
117 **axis in the developing and postnatal hippocampus**
118 To investigate the functions of the *COUP-TFI* and *COUP-TFII* genes in the hippocampus,
119 immunofluorescence staining was first performed to examine their expression in wild-type
120 mice at postnatal month 1 (1M). In both the coronal and sagittal sections, COUP-TFI
121 exhibited a septal/dorsal high-temporal/ventral low expression pattern along the hippocampus
122 (Figure 1Aa, d, c, f, g, j, m, i, l, and o), and its expression is highest in the dorsal CA1 region
123 (Figure 1Aa, d, c, f, j, and l), where place cells are mainly located (O'Keefe & Conway, 1978;
124 O'Keefe & Dostrovsky, 1971), and the dorsal DG, where there are adult neural stem cells
125 (NSCs) (Gould & Cameron, 1996). However, the expression of COUP-TFII was high in the
126 temporal/ventral hippocampus but was barely detected in the septal/dorsal part of the
127 hippocampus (Figure 1Ab, c, e, f, h, i, k, l, n, and o). The dorsal-high COUP-TFI and ventral-
128 high COUP-TFII expression profiles were further verified in the postnatal hippocampi at 1M
129 by western blotting assays (Figure 1Ap, q). At embryonic day 10.5 (E10.5), COUP-TFI was
130 detected in the dorsal pallium (DP) laterally and COUP-TFII was expressed in the MP and
131 CH medially (Figure 1—figure supplement 1Aa-b). At E11.5 and E12.5, the expression of
132 COUP-TFII remained in the CH (Figure 1—figure supplement 1Ac-d, Bb-c). Interestingly,
133 COUP-TFI and -TFII generated complementary expression patterns in the hippocampal
134 primordium with COUP-TFI in the dorsal MP and COUP-TFII in the ventral CH at E14.5

135 (Figure 1—figure supplement 1Ba-f). Additionally, septal/dorsal-high COUP-TFI and
136 temporal/ventral-high COUP-TFII expression patterns were observed at postnatal day 0 (P0)
137 (Figure 1—figure supplement 1Bg-l). The data above revealed that the differential expression
138 patterns of *COUP-TFI* and *-TFII* genes were generated and maintained along the
139 dorsoventral axis in the early hippocampal primordium, the developing and postnatal
140 hippocampus, indicating that they could play distinct roles in the mediation of the
141 morphogenesis and functions of the hippocampus.

142 Next, to investigate the roles of *COUP-TF* genes in the hippocampus, an *RXCre* mouse was
143 used to excise the expression of the *COUP-TFI* and/or *COUP-TFII* genes (Swindell et al.,
144 2006). The deletion efficiency of RXCre recombinase was verified by immunofluorescence
145 assays. Compared with control mice, either *COUP-TFII* or *COUP-TFI* could be excised in
146 the postnatal hippocampus of corresponding single-gene mutants at 1M (Figure 1—figure
147 supplement 1Ca-i). In addition, compared with control mice, both the *COUP-TFI* and *-TFII*
148 genes were almost completely deleted in the hippocampal primordium in mutant mice at
149 E14.5 (Figure 1—figure supplement 1Cj-o). Since the LacZ expression serves as an indicator
150 for the deletion of *COUP-TFII* (Tang et al., 2012), we performed immunofluorescence
151 staining with antibodies against COUP-TFII and LacZ on the sagittal sections of *RXCre/+;*
152 *COUP-TFII*$^{F/+}$ and *RXCre/+; COUP-TFII*$^{F/F}$ mice at E11.5. COUP-TFII was readily detected
153 at the hippocampal primordium of the heterozygous mutant embryo at E11.5 (Figure 1—
154 figure supplement 1Da, c, g); in contrast, the expression of *COUP-TFII* was significantly
155 reduced in the homozygous mutant (Figure 1—figure supplement 1Dd, f, j). In addition,
156 compared with the heterozygous mutant embryo (Figure 1—figure supplement 1Db-c, h), the
157 LacZ signals clearly increased in the hippocampal primordium of the homozygous mutant
158 embryo at E11.5 (Figure 1—figure supplement 1De-f, k), suggesting that RXCre
159 recombinase can efficiently excise the *COUP-TFII* gene in the hippocampal primordium as

160 early as E11.5. Intriguingly, we observed that the expression of *COUP-TFI* increased in the
161 caudal hippocampal primordium of the *COUP-TFII* homozygous mutant embryo at E11.5
162 (Figure 1—figure supplement 1Di, l), indicating that similar to the observations in the early
163 optic cup (Tang et al., 2010), *COUP-TFI* and *-TFII* genes could be partially compensate with
164 each other in the developing hippocampal primordium. All the data above show that RXCre
165 recombinase could efficiently excise *COUP-TFI* and/or *COUP-TFII* in the early developing
166 and postnatal hippocampus.
167

168 **The *COUP-TFII* gene is required for the appropriate morphogenesis of the ventral**
169 **hippocampus but not of the dorsal hippocampus**

170 Given that the *COUP-TFII* gene is highly and specifically expressed in the postnatal ventral
171 hippocampus and the CH of the hippocampal primordium (Figure 1 and Figure 1—figure
172 supplement 1), we asked whether the *COUP-TFII* gene is required for the appropriate
173 morphogenesis of the hippocampus, particularly the ventral hippocampus. To answer this
174 question, we conducted Nissl staining with samples from the *COUP-TFII* single-gene
175 (*RXCre/+*; *COUP-TFII*$^{F/F}$ or *RXCre/+*; *CII*$^{F/F}$) knockout mouse model. In coronal sections,
176 compared with the control at 1M, the septal hippocampus was normal; unexpectedly, an
177 ectopic CA-like region was observed medially in the temporal hippocampus in the *COUP-*
178 *TFII* mutant, where the prospective posterior part of the medial amygdaloid (MeP) nucleus
179 was situated, indicated by the star (Figure 1Ba-f). The presence of the ectopic CA-like region
180 in the ventral but not dorsal hippocampus of the mutant was further confirmed by the
181 presence of the prospective MeP and amygdalohippocampal area (AHi) in sagittal sections,
182 as indicated by the star (Figure 1Bg-l). Furthermore, immunofluorescence assays were
183 performed to verify whether specific lineages of the hippocampus were altered with sagittal
184 sections, in which the subregions of both the dorsal and ventral hippocampus were well

185 displayed and distinguished. Ctip2 is a marker for CA1 pyramidal neurons and DG granule
186 neurons, and HuB is a marker for CA3 pyramidal cells (Sugiyama, Osumi, & Katsuyama,
187 2014). The dorsal hippocampus appeared normal in both the control and mutant mice at 1M
188 (Figure 1Ca-l). Nonetheless, compared with the observations in control mice, an ectopic
189 HuB-positive CA3 pyramidal neuron lineage, indicated by the star, and a duplicated Ctip2-
190 positive CA1 pyramidal neuron lineage, indicated by the arrowhead, were observed in the
191 ventral hippocampal area in the mutant (Figure 1Ca-f, m-r), revealing that there were ectopic
192 CA1 and CA3 lineages in the *COUP-TFII* mutants.
193 Consistent with the previous report (Leid et al., 2004), the expression of Ctip2 was detected
194 in the amygdala including the AHi and posteromedial cortical amygdaloid nucleus (PMCo);
195 in addition, Ctip2 was also highly expressed in the dorsal part of the MeP (MePD) in the
196 control (Figure 1Cb, n).
197 Intriguingly, compared with the controls at 1M, there were ectopic CA domains in the mutant
198 ventral hippocampus with the expense of the Ctip2 positive AHi and MePD amygdaloid
199 nuclei (Figure 1Ce, q), indicated by the arrows. Clearly, all the data above suggested that the
200 *COUP-TFII* gene is necessary to ensure the appropriate morphogenesis of the ventral
201 hippocampus.
202 At early embryonic stages, *COUP-TFII* was preferentially expressed in the CH (Figure 1—
203 figure supplement 1Ab, d, 1Bb, e), the organizer of the hippocampus, and at postnatal 1-
204 month-old (1M) stage, *COUP-TFII* was also highly expressed in some amygdala nuclei such
205 as the AHi and medial amygdaloid nucleus, which are adjacent to the ventral/temporal
206 hippocampus (Figure 1Ae, h, n) (Tang et al., 2012). We would like to investigate the
207 correlation of the CH and/or amygdala anlage with the duplicated ventral hippocampal
208 domains in the *COUP-TFII* mutant in detail in our future study. The observations above
209 suggest that *COUP-TFII* is not only specifically expressed in the ventral hippocampus but is

210 also required for morphogenesis and probably the function of the ventral hippocampus. Since
211 the ventral hippocampus participates in the regulation of emotion and stress, mutations in the
212 *COUP-TFII* gene lead to CHDs, and the formation of the ventral hippocampus is disrupted in
213 *COUP-TFII* mutant mice at 1M, we wondered whether CHD patients with *COUP-TFII*
214 mutations also exhibit symptoms associated with psychiatric disorders such as depression,
215 anxiety, or schizophrenia.
216

217 **The *COUP-TFI* gene is required for the specification and differentiation of the dorsal**
218 **CA1 identity**

219 Next, we asked whether the deletion of the *COUP-TFI* gene by *RXCre* also affected the
220 development of the hippocampus. Consistent with the previous finding in *Emx1Cre/+*;
221 *COUP-TFI*$^{F/F}$ (*Emx1Cre/+*; *CI*$^{F/F}$) mutant mice (Flore et al., 2017), it was the septal/dorsal
222 hippocampus, not the temporal/ventral hippocampus, that was specifically shrunken in both
223 coronal (Figure 2Aa-f) and sagittal sections (Figure 2Ag-i) of *RXCre/+*; *COUP-TFI*$^{F/F}$
224 (*RXCre/+*; *CI*$^{F/F}$) mutant mice. Then, we asked whether the loss of the *COUP-TFI* gene
225 caused abnormal specification and differentiation of hippocampal lineages. Compared with
226 the control mice, *COUP-TFI* mutant mice had fewer HuB-positive CA3 pyramidal neurons,
227 as indicated by the star; intriguingly, Ctip2-positive CA1 pyramidal neurons failed to be
228 detected, as indicated by the arrowhead, with Ctip2-positive DG granule neurons unaltered in
229 the dorsal hippocampus (Figure 2Ba-l). The loss of the dorsal CA1 pyramidal neuron identity
230 in mutant mice was further confirmed by Wfs1, another dorsal CA1 pyramidal neuron-
231 specific marker (Takeda et al., 2001) (Figure 2Ca-r). Nonetheless, the HuB-positive and
232 Ctip2-positive lineages were comparable in the ventral hippocampus between the control and
233 mutant mice (Figure 2Ba-f, m-r), even though the low expression of COUP-TFI was detected
234 there. Indeed, *COUP-TFI* is not only expressed at the highest level in the dorsal CA1 but is

235 also required for the specification and differentiation of dorsal CA1 pyramidal neurons,
236 among which place cells are essential for learning and memory (O'Keefe & Conway, 1978;
237 O'Keefe & Dostrovsky, 1971).

238 Given that dysplasia of the dorsal hippocampus was generated in both the *Emx1Cre* and
239 *RXCre* models (Flore et al., 2017) (Figure 2Aa-l), we asked whether the development of
240 dorsal CA1 pyramidal neurons was also abolished in *Emx1Cre/+*; *COUP-TFI*$^{F/F}$ mutant mice.
241 To answer this question, immunofluorescence staining was conducted first. Compared with
242 that in the control mice, the proportions of either the Wfs1- or Ctip2-positive CA1 domain
243 were reduced in the mutant mice at 3M (Figure 2—figure supplement 1Aa-h), indicating that
244 the differentiation of the dorsal CA1 pyramidal neurons was also compromised in the
245 *Emx1Cre* model, although it was less severe than that in the *RXCre* model. To make our
246 findings more consistent with previous studies, we further conducted experiments with the
247 *Emx1Cre* model. Afterward, to investigate the fine structure of the dorsal CA1 pyramidal
248 neurons, Golgi staining was performed. Compared with those of control mice, the numbers of
249 secondary dendrites and branch points of both the apical and basal dendrites were
250 significantly reduced in the dorsal CA1 pyramidal neurons of mutant mice at 3M (Figure 2—
251 figure supplement 1Ba-e). Then, the dorsal hippocampus-related spatial learning and memory
252 behavior test, the Morris water maze, was performed (Vorhees & Williams, 2006). Consistent
253 with a previous report (Flore et al., 2017), spatial learning and memory function was
254 significantly impaired in adult *Emx1Cre*/+; *COUP-TFI*$^{F/F}$ mice, compared with the control
255 mice (Figure 2—figure supplement 1C). The data above suggest that *COUP-TFI* is vital for
256 the morphogenesis, lineage specification, and spatial learning and memory of the dorsal
257 hippocampus, and particularly, the compromised dorsal CA1 lineage could contribute to the
258 phenotypes associated with neurodevelopmental disorders, including ID or ASD.
259

260 **The *COUP-TFI* and *-TFII* genes coordinate to ensure the genesis of the hippocampus**

261 Given that the loss of either *COUP-TFI* or *-TFII* leads to dysplasia of the dorsal or ventral
262 hippocampus, respectively, we asked whether these genes compensate for each other to
263 regulate the morphogenesis of the hippocampus. To answer this question, the *RXCre/+*;
264 *COUP-TFI*$^{F/F}$; *COUP-TFII*$^{F/F}$ (*RXCre/+*; *CI*$^{F/F}$; *CII*$^{F/F}$) double-mutant mouse was generated,
265 and a few homozygous double-gene mutant mice survived for approximately 3 weeks (3W).
266 Nonetheless, the reason for the lethality of the double-mutant mice is still unknown. Nissl
267 staining data showed that compared with that of control mice, the septal hippocampus was
268 severely shrunken, as indicated by the star, and the temporal hippocampus was barely
269 observed in the double-mutant mouse brains (Figure 3Aa-h). Unexpectedly, an ectopic
270 nucleus was observed in the region of the prospective temporal hippocampus, indicated by
271 the arrowhead, in the double-mutant mice (Figure 3Ag-h). In addition, compared with those
272 of controls, the regions with HuB-positive CA3 pyramidal neurons and Ctip2-positive or
273 Prox1-positive DG granule neurons were diminished in the double mutants; in particular,
274 Ctip2-positive dorsal CA1 pyramidal neurons could not be detected in the double mutants
275 (Figure 3Ba-l). Furthermore, compared with the domains of controls, no HuB-positive, Ctip2-
276 positive, or Prox1-positive domains could be detected in the prospective temporal
277 hippocampus in the double mutants (Figure 3Ca-l). The results above suggest that the *COUP-*
278 *TFI* and *COUP-TFII* genes coordinate with each other to mediate the appropriate
279 morphogenesis of the entire hippocampus.

280

281 ***COUP-TF* genes and adult neurogenesis in the hippocampus**

282 Given that the *COUP-TFI* or *-TFII* gene was highly expressed in the dorsal or ventral DG,
283 respectively (Figure 1A), and that RXCre recombinase could efficiently delete either gene in
284 the DG (Figure 1—figure supplement 1Ca-i), we asked whether the loss of the *COUP-TFI*

285 or/and -*TFII* gene in the DG would affect hippocampal adult neurogenesis. To answer this
286 question, the ventral DG, dorsal DG, and septal DG were chosen to perform
287 immunofluorescence assays in the *COUP-TFII* mutant, *COUP-TFI* mutant, and double
288 mutant models, respectively. Adult NSCs in the subgranular zone (SGZ) of the DG express
289 both GFAP and Nestin, and newborn granule neurons express Dcx (Gao, Arlotta, Macklis, &
290 Chen, 2007). The numbers of NSCs and newborn neurons in the SGZ of the DG were
291 comparable between control mice and either the *COUP-TFII* or *COUP-TFI* mutant mice
292 (Figure 3—figure supplement 1Aa-p, Ba-h); nonetheless, compared with those of control
293 mice, the numbers of the NSCs and newborn granule neurons in the SGZ of the DG were
294 reduced in the double mutants (Figure 3—figure supplement 1Aq-x, Bi-l), and the reduction
295 in both lineages was significant (Figure 3—figure supplement 1Ca, b). The data above
296 suggest that *COUP-TF* genes may coordinate with each other to execute essential functions
297 for appropriate hippocampal adult neurogenesis in the DG.
298

299 **Hippocampal trisynaptic connectivity was impaired in postnatal *COUP-TFII* single-,**
300 ***COUP-TFI* single-, and double-mutant mice at about 1M**

301 Given that dysplasia of the hippocampus was observed in all three mouse models, we asked
302 whether the connectivity of the hippocampal trisynaptic circuit associated with the DG, CA3,
303 and CA1 regions (Amaral, 1993) was normal in these models. To answer this question, the
304 components of the trisynaptic circuit were characterized in the ventral hippocampus of
305 *COUP-TFII* mutants, the dorsal hippocampus of *COUP-TFI* mutants, and the septal
306 hippocampus of double mutants. Calretinin is a marker of mossy cells, Calbindin is a marker
307 of mossy fibers, and SMI312 is a marker of Schafer collaterals (Flore et al., 2017). Compared
308 with those of controls (Figure 4Aa, b, e, f, i, and j), the numbers of Calretinin-positive mossy
309 cells were reduced, Calbindin-positive mossy fibers were longer but thinner, and SMI312-

310 positive Schafer collaterals were thinner and discontinued in the ventral hippocampus of
311 *COUP-TFII* mutants at 1M (Figure 4Ac, d, g, h, k, and l). In addition, similar to the previous
312 report (Flore et al., 2017), the numbers of Calretinin-positive mossy cells were decreased,
313 Calbindin-positive mossy fibers were shorter and thinner, and SMI312-positive Schafer
314 collaterals were barely detected in the dorsal hippocampus of *COUP-TFI* mutants (Figure
315 4Ac, d, g, h, k, and l), compared with those of controls at 1M (Figure 4Ba, b, e, f, i, and j).
316 Moreover, compared with those of control mice (Figure 4Ca, b, e, f, i, and j), the numbers of
317 Calretinin-positive mossy cells were reduced; both Calbindin-positive mossy fibers and
318 SMI312-positive Schafer collaterals were barely detected in the prospective septal
319 hippocampus of the double mutants at 3W (Figure 4Cc, d, g, h, k, and l). Clearly, without
320 both *COUP-TF* genes, the connectivity of the hippocampal trisynaptic circuit was abolished
321 more severely. The observations above revealed that the formation of the trisynaptic circuit,
322 which is one of the fundamental characteristics of hippocampal neurophysiology (Basu &
323 Siegelbaum, 2015), was abnormal in all three mouse models, indicating that both the
324 morphology and functions of the hippocampus are most likely compromised in the loss of the
325 *COUP-TFI* and/or *COUP-TFII* gene.
326

327 **The expression of several essential regulatory genes associated with early hippocampal**
328 **development was abnormal in double mutants**

329 Given that the hippocampus was almost completely diminished in double mutants, we asked
330 how *COUP-TF* genes participated in the regulation of the early morphogenesis of the
331 hippocampus. To answer this question, total RNA isolated from the whole telencephalons of
332 control (n=5) and double-mutant-(n=3) embryos at E11.5 was used to generate cDNA, and
333 then real-time quantitative PCR (RT-qPCR) assays were performed. As expected, compared
334 with that of control mice, the expression of *COUP-TFI* and *COUP-TFII* was reduced

335 significantly in the double mutant mice (Figure 5A). Then, we mainly focused on the intrinsic
336 regulatory networks by analyzing the expression profiles of two groups of transcription factor
337 genes. The *Foxg1*, *Gli3*, *Lhx2*, *Otx1, Otx2*, and *Pax6* genes, which are highly related to the
338 early patterning of the dorsal telencephalon (Hébert & Fishell, 2008), were in the first group;
339 *Axin2*, *Emx1*, *Emx2*, *Lef1*, *Lhx5*, and *Tcf4* genes, which are associated with early
340 hippocampal development (Galceran et al., 2000; Moore & Iulianella, 2021; Tole et al., 2000;
341 Yoshida et al., 1997; Zhao et al., 1999), were in the other group. The expression of the *Foxg1*,
342 *Gli3*, *Lhx2*, *Otx1, Otx2*, and *Pax6* genes was comparable between the controls and double
343 mutants (Figure 5A), indicating that the early patterning of the dorsal telencephalon is largely
344 unaltered. Compared with that of control mice, the expression of the *Axin2*, *Emx2*, *Lef1*, and
345 *Tcf4* genes was normal in the double mutants; interestingly, the expression of the *Emx1* and
346 *Lhx5* transcripts was decreased significantly in the double mutants at E11.5 compared to that
347 in control mice (Figure 5A). Consistent with the downregulated expression of *Lhx5*
348 transcripts in the double mutant, the expression of the Lhx5 protein was reduced in the CH in
349 the double mutants at E11.5; moreover, the number of Lhx5-positive Cajal-Retzius cells
350 decreased in the double mutant embryos at E11.5, E13.5 and E14.5 (Figure 5Ba-d, a'-d', a''-
351 d'', i-l, i'-l', q-t, q'-t'). The expression of *Lhx2* was expanded ventrally into the choroid
352 plexus in the *Lhx5* null mutant mice (Zhao et al., 1999), indicating that *Lhx5* could inhibit
353 *Lhx2* expression locally. Consistent with RT-qPCR data, the expression of Lhx2 was
354 comparable between the control and double-mutant mice at E11.5 (Figure 5Be-h, e'-h').
355 Interestingly, the expression of the Lhx2 protein was increased in the hippocampal
356 primordium in the *COUP-TF* double-mutant mice at E13.5 and E14.5 (Figure 5Bm-p, m'-p',
357 u-x, u'-x'). The upregulation of Lhx2 expression is most likely associated with the reduced
358 expression of the *Lhx5* gene.

359 Next, we asked whether neural precursor cells (NPCs), intermediate progenitor cells (IPCs),
360 or newborn neurons were affected in the early development of the hippocampus in double-
361 mutant mice. Sox2 is a marker for NPCs, Tbr2 is a marker for IPCs, and NeuroD1 is a marker
362 for newborn neurons (Yu, Marchetto, & Gage, 2014). The expression of Sox2 in the
363 hippocampal regions was comparable between the control and double-mutant mice at E14.5
364 (Figure 5Ca-d, a'-d'), indicating that the generation of NPCs was normal. Nevertheless,
365 compared with the control embryos, the numbers of Tbr2-positive IPCs and NeuroD1-
366 positive newborn neurons were reduced in the double-mutant embryos (Figure 5Ce-l, e'-l'),
367 and the reduction was significant (Figure 5D). Our observations were consistent with
368 previous findings in *Lhx5* null mutant mice that the specification of the hippocampal NPCs
369 was normal, but the later differentiation event was abolished (Zhao et al., 1999). All the data
370 above suggest that *COUP-TF* genes may cooperate to ensure the early morphogenesis of the
371 hippocampus by regulating the appropriate expression levels of *Lhx5* and *Lhx2* genes.
372 Nevertheless, we could not exclude other possibilities that *COUP-TF* genes could also
373 participate in the modulation of hippocampal development through *Emx1* or other genes.
374

375 **Discussion**

376 In our present study, we observed dorsal-high COUP-TFI and ventral-high COUP-TFII
377 expression profiles in the postnatal hippocampus. The deletion of the *COUP-TFII* gene led to
378 duplicated CA1 and CA3 domains of the ventral hippocampus. The loss of *COUP-TFI*
379 resulted in the failed specification and differentiation of the dorsal CA1 pyramidal neuron
380 lineage with a diminished dorsal hippocampus. Furthermore, the deficiency of both *COUP-*
381 *TF* genes caused atrophy of almost the entire hippocampus, accompanied by compromised
382 generation of the CA1, CA3, and DG identities. In addition, the dorsal trisynaptic
383 components, ventral trisynaptic components, or entire trisynaptic components were abolished

384 in the corresponding *COUP-TFI* gene mutant, *COUP-TFII* gene mutant, or *COUP-TFI/-TFII*
385 double-gene mutant mice. Moreover, *COUP-TF* genes may cooperate to ensure the
386 appropriate morphogenesis and function of the hippocampus by regulating the *Lhx5-Lhx2*
387 axis.
388
389 **1. *COUP-TFII* governs the distinct characteristics of the ventral hippocampus**
390 Sixty years ago, the pioneering work of Milner and her colleagues discovered the essential
391 role of the hippocampus in declarative memory (Penfield & Milner, 1958; Scoville & Milner,
392 1957). Recently, accumulating evidence has supported the Moser theory that the
393 hippocampus is a heterogeneous structure with distinct characteristics of gene expression,
394 connectivity, and function along its dorsoventral axis (Bast, 2007; Fanselow & Dong, 2010;
395 Moser & Moser, 1998; Strange et al., 2014). The dorsal hippocampus marked in blue, in
396 which gene expression is similar to the neocortex, serves the "cold" cognitive function
397 associated with declarative memory and spatial navigation, and the ventral hippocampus
398 marked in red, in which gene expression is close to the hypothalamus and amygdala,
399 corresponds to the "hot" affective states related to emotion and anxiety (Figure 5—figure
400 supplement 1). The ventral hippocampus generates direct connectivity with the amygdala,
401 hypothalamus, medial prefrontal cortex (mPFC), and olfactory bulb (Cenquizca & Swanson,
402 2007; Hoover & Vertes, 2007; Kishi et al., 2000; Pitkanen et al., 2000; Roberts et al., 2007).
403 Nonetheless, thus far, the molecular and cellular mechanism of how the morphogenesis,
404 connectivity, and function of the ventral hippocampus is achieved has been largely unclear.
405 *COUP-TFII*, a nuclear receptor gene associated with heart disease (High et al., 2016), was
406 highly and exclusively expressed in the ventral hippocampus in 1-month-old mice and was
407 expressed ventrally in the CH of the hippocampal primordium in mouse embryos (Figure 1,
408 Figure 1—figure supplement 1, Figure 5Ea), indicating that the *COUP-TFII* gene may

409 participate in the regulation of the development and function of the ventral hippocampus.
410 First, deficiency of the *COUP-TFII* gene led to the duplication of the CA1 and CA3 domains
411 of the ventral hippocampus but not the dorsal hippocampus, which was confirmed both
412 morphologically and molecularly (Figure 1). Second, the formation of the trisynaptic circuit
413 was specifically abolished in the ventral hippocampus of *COUP-TFII* mutants (Figure 4),
414 indicating that the intrahippocampal circuit, information transfer, and function of the ventral
415 hippocampus could be compromised. Third, the ventral hippocampus generates neural
416 circuits with the mPFC, amygdala, nucleus accumbens, and hypothalamus, which are
417 associated with anxiety/behavioral inhibition, fear processing, pleasure/reward seeking, and
418 the neuroendocrine system, respectively (Anacker & Hen, 2017; Baik, 2020; Bryant &
419 Barker, 2020; Cenquizca & Swanson, 2007; Herman et al., 2016; Kishi et al., 2000; O'Leary
420 & Cryan, 2014; Pitkanen et al., 2000). These ventral hippocampal projections may be
421 important for processing information related to emotion and anxiety. Intriguingly, our
422 previous studies revealed that *COUP-TFII* is required for the development of the
423 hypothalamus, amygdala, and olfactory bulb (S. Feng et al., 2017; Tang et al., 2012; X. Zhou
424 et al., 2015), all of which generate functional neural circuits with the ventral hippocampus
425 (Fanselow & Dong, 2010). Particularly, both the hypothalamus and amygdala are also
426 diminished in *RXCre*/+; *COUP-TFII*$^{F/F}$ mutant mice (S. Feng et al., 2017; Tang et al., 2012),
427 indicating that their interconnectivities with the ventral hippocampus are abnormal. Thus, all
428 the findings above suggest that *COUP-TFII* is a novel and essential intrinsic regulator that
429 controls the morphogenesis, connectivity, and function of the ventral hippocampus.
430 Given that mutations of *COUP-TFII* are highly associated with CHDs and are required for
431 the distinct characteristics of the ventral hippocampus, we wondered whether CHD patients
432 carrying mutations of *COUP-TFII* also display symptoms of psychiatric disorders, such as
433 depression, anxiety, or schizophrenia, related to the ventral hippocampus. In our future study,

434 we would like to generate hippocampus-specific or hippocampal subdomain-specific
435 conditional knockout models to dissect distinct roles of the *COUP-TFII* gene in the
436 hippocampus, particularly in the ventral hippocampus, in detail.
437

438 **2. The *COUP-TFI* gene is required for the specification and differentiation of dorsal**
439 **CA1 pyramidal neurons**

440 The expression of *COUP-TFI*, another orphan nuclear receptor gene associated with
441 neurodevelopmental disorders (Bertacchi et al., 2020; Bosch et al., 2014; Contesse et al.,
442 2019), is high in the dorsal MP of the hippocampal primordium and is higher in the dorsal
443 hippocampus than in the ventral hippocampus (Figure 1, Figure 1—figure supplement 1,
444 Figure 5Ea) (Flore et al., 2017). Consistent with previous observations in *Emx1Cre/+*;
445 *COUP-TFI*$^{F/F}$ mutant mice (Flore et al., 2017), the dorsal hippocampus but not the ventral
446 hippocampus was specifically shrunken in *RXCre/+; COUP-TFI*$^{F/F}$ mice (Figure 2, Figure
447 5—figure supplement 1). *COUP-TFI* is expressed at the highest level in dorsal CA1
448 pyramidal neurons (Figure 1), indicating that the *COUP-TFI* gene may play a role in the
449 specification and differentiation of dorsal CA1 pyramidal neurons. As expected, the
450 expression of Ctip2 and Wfs1, two markers for dorsal CA1 pyramidal neurons, could not be
451 detected in the prospective dorsal CA1 domain in *RXCre/+*; *COUP-TFI*$^{F/F}$ mutant mice
452 (Figure 2); furthermore, *Emx1Cre/+*; *COUP-TFI*$^{F/F}$ mutant mice partially phenocopied the
453 compromised development of the dorsal CA1 lineage (Figure 2—figure supplement 1). It
454 seems that the spatiotemporal activity of RXCre recombinase is better or broader than that of
455 the Emx1Cre recombinase during the critical period of the specification of the dorsal CA1
456 pyramidal neuron identity. In addition, the Golgi staining assay revealed that the
457 development of the dendrites of the dorsal CA1 pyramidal neurons was abnormal (Figure 2—
458 figure supplement 1). All the observations above indicate that the *COUP-TFI* gene is not only

459 necessary for the morphogenesis of the dorsal hippocampus but is also required for the
460 specification and differentiation of the dorsal CA1 pyramidal neurons, among which there are
461 place cells. The identification of place cells fifty years ago was one of the most important
462 breakthroughs in understanding the role of the hippocampus in memory (O'Keefe &
463 Dostrovsky, 1971). Except for spatial information, place cells in the dorsal CA1 may also
464 encode nonspatial representations, such as time (Eichenbaum, 2017; Lisman et al., 2017).
465 Notably, 95% of patients carrying *COUP-TFI* mutations are associated with ID. Here, our
466 observations support the notion that the *COUP-TFI* gene is a novel intrinsic regulator that
467 specifies the dorsal CA1 pyramidal cell identity, which will benefit the understanding of both
468 neurophysiological functions of the hippocampus and the etiology of NDD including ID and
469 ASD.
470

471 **3. *COUP-TFI* and *-TFII* cooperate to ensure the appropriate morphogenesis of the**
472 **hippocampus by regulating the *Lhx5-Lhx2* axis in mice**

473 In wild-type mice, *COUP-TFI* and *-TFII* genes generated complementary expression profiles
474 in the embryonic hippocampal primordium with *COUP-TFI* in the dorsal MP, marked in
475 green; *COUP-TFII* in the ventral CH, marked in red (Figure 5Ea, Figure 1—figure
476 supplement 1); and in the postnatal hippocampus with high-COUP-TFI expression in the
477 dorsal, marked in green; and high-COUP-TFII expression in the ventral, marked in red
478 (Figure 5Ea, Figure 1). These findings indicated that *COUP-TF* genes may coordinate to
479 regulate hippocampal development. Indeed, as discussed above, the loss of either *COUP-TFI*
480 or *-TFII* only leads to dysplasia of the dorsal hippocampus (Flore et al., 2017) (Figure 2,
481 Figure 2—figure supplement 1) or ventral hippocampus (Figure 1), respectively; intriguingly,
482 while both genes are efficiently excised by *RXCre* in the hippocampal primordium (Figure
483 1—figure supplement 1), more severely shrunken hippocampi developed in the 3-week-old

484 double knockout mice (Figure 3). The dosage-dependent severity of hippocampal
485 abnormalities suggested that two nuclear receptor genes, *COUP-TFI* and *-TFII* could
486 cooperate with each other to execute an essential and intrinsic function in the development of
487 the hippocampus.

488 It is known that both extrinsic signals and intrinsic factors participate in the regulation of the
489 early development of the hippocampus. Notably, mutations of *Wnt3a* and *Lef1* eliminate the
490 entire hippocampus (Galceran et al., 2000; S. M. Lee et al., 2000). Given that the expression
491 of *Axin2*, *Lef1* and *Tcf4*, three Wnt-responsive transcription factor genes, was not altered in
492 the *COUP-TF* double mutant (Figure 5A), it is unlikely that abnormal Wnt signaling is the
493 cause of the compromised hippocampus. *Lhx5* is specifically expressed in the hippocampal
494 primordium and is required for the morphogenesis of the hippocampus (Zhao et al., 1999).
495 *Lhx2* is necessary for hippocampal development by repressing cortical hem fate (Mangale et
496 al., 2008; Monuki et al., 2001). Agenesis of the hippocampus is observed in either *Lhx5* or
497 *Lhx2* null mutant mice, and these genes particularly repress each other (Hébert & Fishell,
498 2008; Mangale et al., 2008; Roy et al., 2014; Zhao et al., 1999), indicating that the proper
499 expression levels of *Lhx5* and *Lhx2* genes are critical to maintain the appropriate
500 development of the hippocampus (Figure 5Eb). The transcriptional and protein expression
501 levels of *Lhx5* but not *Lhx2* were first reduced in the hippocampal primordium of *COUP-TF*
502 double-mutant mice at E11.5; later, enhanced expression of the Lhx2 protein was detected in
503 the hippocampal primordium of double-mutant mice at E13.5 and E14.5 (Figure 5A-B).
504 Moreover, the number of Lhx5-positive Cajal-Retzius cells was clearly reduced in the double
505 mutant embryos at E11.5, E13.5 and E14.5; consistent with the observations in the *Lhx5* null
506 mutant (Li et al., 2021; Miquelajáuregui et al., 2010), the generation of Sox2-positive
507 hippocampal NPCs was not affected, but the development of Tbr2-positive IPCs and
508 NeuroD1-positive newborn neurons was abnormal in *COUP-TF* double-mutant mice (Figure

509 5). Thus, our findings reveal a novel intrinsic regulatory mechanism that *COUP-TFI* and
510 *COUP-TFII*, two disease-associated nuclear receptor genes, may cooperate with each other to
511 ensure proper hippocampal morphogenesis by regulating the *Lhx5-Lhx2* axis. Intriguingly,
512 compared with the adult *Emx1Cre/+*; *COUP-TFI*$^{F/F}$ mutant mice, the hippocampus was much
513 smaller in the adult *Emx1Cre/+*; *COUP-TFI*$^{F/F}$; *COUP-TFII*$^{F/F}$ double-gene mutant mice;
514 nevertheless, both the dorsal and ventral hippocampus were readily detected in double-gene
515 mutants with *Emx1Cre* (our unpublished observations). In addition, the discrepancy between
516 the shrunken dorsal hippocampus associated with the loss of *COUP-TFI* and the duplicated
517 CA domains of the ventral hippocampus associated with the deficiency of *COUP-TFII*
518 suggested that the regulatory network related to *COUP-TF* genes during the early
519 morphogenesis of the hippocampus could be much more complicated than suspected and
520 should be investigated in our future study.
521
522 **4. *COUP-TF* genes are imperative for the formation of the trisynaptic circuit**
523 The hippocampus and entorhinal cortex (EC) are interconnected through various neural
524 circuits to mediate the flow of the information associated with declarative memory (Basu &
525 Siegelbaum, 2015). Both direct and indirect glutamatergic circuits are involved in the relay of
526 information from the EC to the hippocampal CA1, and the trisynaptic pathway is the most
527 well-characterized indirect circuit. The EC sends sensory signals from association cortices
528 via the perforant path to the DG, then the DG granule cells send excitatory mossy fiber
529 projections to CA3 pyramidal neurons, and CA3 pyramidal neurons project to CA1 via the
530 Schaffer collaterals (H. Lee, GoodSmith, & Knierim, 2020). Consistent with the high
531 expression of COUP-TFI in the dorsal hippocampus and COUP-TFII in the ventral
532 hippocampus (Figure 1), the dorsal trisynaptic circuit is specifically damaged in *COUP-TFI*
533 mutants, as is the ventral trisynaptic circuit in *COUP-TFII* mutant mice. Moreover, the

534 hippocampal trisynaptic circuit was almost completely absent in the double mutants (Figure 4,
535 and our unpublished observations). The information transfer associated with the trisynaptic
536 circuits should be abolished particularly in the dorsal and/or the ventral hippocampus in the
537 above corresponding genetic mouse models. Interestingly, *COUP-TFI* is also required to
538 specify the medial EC cell fate (J. Feng et al., 2021). Therefore, the impaired formation and
539 function of trisynaptic circuits could be caused by the abnormal development of CA1, CA3,
540 DG or EC lineages. Nonetheless, given that newborn granule neurons are continuously
541 generated in the adult DG to integrate into the existing neural circuits essential for declarative
542 memory (Toda, Parylak, Linker, & Gage, 2019; Tuncdemir, Lacefield, & Hen, 2019) and that
543 hippocampal adult neurogenesis was severely compromised in the *COUP-TF* double mutant
544 (Figure 3—figure supplement 1), we could not exclude the possibility that impaired adult
545 neurogenesis may also contribute to the malformation and impaired function of the
546 trisynaptic pathway in double mutants.
547
548 The hippocampus is heterogeneous along its dorsoventral axis, and either the dorsal or
549 ventral hippocampus generates unique and distinguishable characteristics of gene expression
550 and connectivity, which enable the hippocampus to execute an integrative function from the
551 encoding and retrieval of certain declarative memory to adaptive behaviors. Lesions of the
552 dorsal hippocampus, which are essential for the cognitive process of learning and memory,
553 lead to amnesia and ID; while damage to the ventral hippocampus, which is central for
554 emotion and affection, is highly associated with psychiatric disorders including depression,
555 anxiety, and schizophrenia. Our findings in this study reveal novel intrinsic mechanisms by
556 which two nuclear receptor genes, *COUP-TFI* and *-TFII*, which are associated with NDD or
557 CHD, converge to govern the differentiation and integration of the hippocampus along the
558 dorsoventral axis morphologically and functionally. Furthermore, our present study provides

559 novel genetic model systems to investigate the crosstalk among the hippocampal complex in
560 gene expression, morphogenesis, cell fate specification and differentiation, connectivity,
561 functions of learning/memory and emotion/anxiety, adaptive behaviors, and the etiology of
562 neurological diseases. Nevertheless, many enigmas, such as whether and how the
563 abnormalities of either the dorsal or ventral hippocampus affect the characteristics of the
564 other, remain unsolved. In addition to the excitatory lineages and circuits, interneurons and
565 inhibitory circuits play vital roles in maintaining the plasticity and functions of the
566 hippocampus. We also wonder whether and how defects in interneurons and inhibitory
567 circuits could contribute to the compromised morphogenesis, connectivity, and functions of
568 the hippocampus and the etiology of psychiatric and neurological conditions including ID,
569 ASD, depression, anxiety, and schizophrenia.
570
571 **Materials and Methods**

572 **Animals**

573 *COUP-TFI-floxed* mice, *COUP-TFII-floxed* mice, *RXCre* mice and *Emx1Cre* mice used in
574 the study were of the C57B6/129 mixed background. The noon of vaginal plug day was set as
575 the embryonic day 0.5 (E0.5). All animal protocols were approved by the Animal Ethics
576 Committee of the Shanghai Institute of Biochemistry and Cell Biology. All methods were
577 performed in accordance with the relevant guidelines and regulations. Only the littermates
578 were used for the comparison.
579

580 **Nissl staining**

581 We used xylene to dewax paraffin sections, followed by rinsing with 100%, 95%, and 70%
582 ethanol. The slides were stained in 0.1% Cresyl Violet solution for 25 mins. Then the
583 sections were washed quickly in the water and differentiated in 95% ethanol. We used 100%

584 ethanol to dehydrate the slides, followed by rinsing with the xylene solution. Finally, the
585 neutral resin medium was used to mount the slides.
586
587 **Immunohistochemical (IHC) staining**
588 The paraffin sections were dewaxed and rehydrated as described above for Nissl staining.
589 The slides were boiled in 1×antigen retrieval solution (DAKO) under microwave conditions
590 for 15 min. After cooled to room temperature (RT), the slides were incubated with 3% H2O2
591 for 30 min. Then, the slides were treated with blocking buffer for 60 min at RT and then
592 incubated with the primary antibody in the hybridization buffer (10×diluted blocking buffer)
593 overnight (O/N) at 4 °C. The next day, the tyramide signal amplification kit (TSA)
594 (Invitrogen) was used according to the manufacturer's protocol. After being incubated with
595 1%TSA blocking buffer, the sections were treated with a biotinylated secondary antibody for
596 60 min at RT. After being washed with 1×PBS three times, the slides were incubated with
597 1×HRP-conjugated streptavidin for 1 h. Next, the tyramide working solution was prepared,
598 including the 0.15‰ H_2O_2 in distilled water, the 100×diluted tyramide substrate solution
599 (tyramide-488 or tyramide-594), and the amplification buffer. The sections were incubated
600 with the working solution for 10 min. Then the slides were counterstained with DAPI and
601 mounted with the antifade mounting medium (Southern Biotech) (S. Feng et al., 2017; Zhang
602 et al., 2020). Finally, the sections were observed and images were captured with a digital
603 fluorescence microscope (Zeiss).
604 The following primary antibodies were used in the study: mouse anti-COUP-TFI (1:1000,
605 R&D), mouse anti-COUP-TFII (1:2000, R&D), rabbit anti-HuB (1:500, Abcam), rat anti-
606 Ctip2 (1:500, Abcam), rabbit anti-Wfs1 (1:500, ProteinTech), goat anti-Prox1 (1:500, R&D),
607 rabbit anti-Calretinin (1:500, Sigma), rabbit anti-Calbindin (1:500, Swant), mouse anti-
608 SMI312(1:200, Covance), rabbit anti-Sox2 (1:500, Affinity BioReagents), rat anti-Tbr2

609 (1:500,Thermo Fisher), goat anti-NeuroD1 (1:200, Santa Cruz), goat anti-Lhx2 (1:200, Santa
610 Cruz), goat anti-Lhx5 (1:200, R&D), goat anti-β-galactosidase (LacZ) (1:400, Biogenesis),
611 mouse anti-GFAP(1:500, Sigma), rabbit anti-Nestin (1:200, Santa Cruz), goat anti-Dcx
612 (1:500, Santa Cruz). The following secondary antibodies were used in the study: donkey anti-
613 mouse (Abboud, Bar, Rosenfeld, Ring, & Glass, 1996) IgG biotin-conjugated (1:400,
614 JacksonImmuno), donkey anti-rabbit IgG biotin-conjugated (1:400, JacksonImmuno), donkey
615 anti-goat IgG biotin-conjugated (1:400, JacksonImmuno), donkey anti-rat IgG biotin-
616 conjugated (1:400, JacksonImmuno).
617
618 **Western blotting**
619 We homogenized the isolated dorsal and ventral hippocampus tissues from 1-month-old mice
620 respectively in the RIPA buffer (Applygen) with protease inhibitor cocktail (Sigma) and
621 phosphatase inhibitors (Invitrogen) and then centrifuged at the speed of 12,000 rpm for 30
622 mins. We collected the supernatants and analyzed the total concentrations by the BCA kit
623 (Applygen). Gradient SDS-PAGE gels were used to separate the same amounts of protein
624 sample (40 μg/lane), and then the proteins were transferred to the PVDF membranes
625 (Millipore). After being blocked by the 3% BSA (Sigma) for 2h, the membranes that
626 contained proteins were incubated by primary antibodies at 4 °C O/N. The membranes were
627 rinsed with 1×PBST three times for 10 mins and then treated with biotinylated secondary
628 antibodies for 2h at RT. After washing with 1×PBST, membranes were treated with the HRP-
629 conjugated streptavidin for 1h at RT. Finally, we used the chemiluminescence detection
630 system (Tanon) to detect the bands. The density of the protein band was analyzed by the
631 software Image J.
632 The primary antibodies were used in the experiment as below: mouse anti-COUP-TFI
633 (1:2000, R&D), rabbit anti-COUP-TFII (1:3000, R&D). The following secondary antibodies

634 were applied in the study, including goat anti-mouse IgG biotin-conjugated (1:1000, KPL),
635 goat anti-rabbit IgG biotin-conjugated (1:1000, KPL).
636
637 **Golgi staining**
638 Deep anesthesia was performed before sacrificing the control and mutant mice, and the brains
639 were immediately isolated. The FD rapid GolgiStain kit (FD NeuroTech) was used to process
640 the brain tissue samples, which were immersed in an equal volume of immersion solution
641 mixed with solutions A and B and stored in the dark for two weeks at RT. At least 5mL of
642 immersion solution was used for each cubic meter of the tissue. To achieve the best results,
643 the container of tissue was gently swirled from side to side twice a week during the
644 incubating period. Afterwards, the brain tissue was transferred to solution C in the dark at RT
645 for at least 72 hours (up to 1 week). Finally, the tissues were cut into 100 μm thick slices with
646 a cryostat at -20°C to -22°C and transferred to gelatin-coated microscope slides containing
647 solution C using a sample retriever. The slices were dried naturally at RT. The concrete
648 staining procedure of the kit was followed using the manufactory's protocol. Then, the
649 sections were rinsed twice with double-distilled water for 4 minutes each time. The slices
650 were placed in a mixture of one volume of solution D, one volume of solution E, and two
651 volumes of double distilled water for 10 minutes and were rinsed twice with distilled water
652 for 4 minutes each time. The sections were later dehydrated in 50%, 75%, and 95% ethanol
653 for 4 minutes respectively. Next, the slices were dehydrated in 100% ethanol 4 times for 4
654 minutes each time. Finally, the sections were cleared in xylene and mounted with a neutral
655 resin medium.
656
657 **Morris water maze**

658 By recording the time spent by the mice swimming in the water tank and finding the escape
659 platform hidden underwater, and the swimming trajectory, the Morris water maze test can
660 objectively reflect the spatial learning and memory ability of the mice. We poured tap water
661 into the water maze tank and added an appropriate amount of well-mixed, milky white food
662 dye. The height of the liquid level was about 1 cm higher than the escape platform, and the
663 water temperature was kept at about 25±1℃. At the same time, four markers of different
664 shapes were pasted on the four directions of the inner wall above the water tank to distinguish
665 different directions. The Morris water maze test was divided into the training phase and the
666 probe trial phase. The training phase lasted for 6 days, 4 times a day, and the interval between
667 each training was about 30 minutes. During training, the mice were placed into the tank from
668 the entry points of four different quadrants facing the inner wall, and their latency was
669 recorded from the time they entered the water to the time they found a hidden underwater
670 platform and stood on it. After the mouse found the platform, we let it stay on the platform
671 for 10 seconds before removing it. If the mouse failed to discover the platform 60 seconds
672 after entering the water, it was guided to find the platform and left to stay for 10 seconds.
673 Each mouse was placed into the water tank from four water entry points and recorded as one
674 training session. The probe trial was carried out on the seventh day, and the underwater
675 platform was removed. Each experimental mouse was put into the water tank at the same
676 water entry point and allowed to move for 60 seconds. The time that each mouse spent in the
677 quadrant, where the platform was originally placed, was recorded.
678

679 **RNA isolation and quantitative real-time PCR**

680 Total RNAs were prepared from the whole telencephalon of the control (n=5) and double
681 mutant (n=3) mice at E11.5 respectively, with the TRIzol Reagent (Invitrogen) by following
682 the manufactory's protocol. Reverse-transcription PCR and real-time quantitative PCR assays

683 were performed as described previously (Tang et al., 2012). A student's t-test was used to
684 compare the means of the relative mRNA levels between the control group and mutant group.
685 Primer sequences are as follows:
686 *Axin2-f*, 5'-*ctgctggtcaggcaggag*-3', *Axin2-r*, 5'-*tgccagtttctttggctctt*-3'; *Coup-tfI-f*, 5'-
687 *caaagccatcgtgctattca*-3', *Coup-tfI-r*, 5'-*cctgcaggctttcgatgt*-3'; *Coup-tfII-f*, 5'-*cctcaaagtgggcatgagac*-
688 3', *Coup-tfII-r*, 5'-*tgggtaggctgggtaggag*-3'; *Emx1-f*, 5'-*ctctccgagacgcaggtg*-3', *Emx1-r,* 5'-
689 *ctcagactccggcccttc*-3'; *Emx2-f*, 5'-*cacgcttttgagaagaacca*-3', *Emx2-r,* 5'-*gttctccggttctgaaacca*-3';
690 *Foxg1-f*, 5'-*gaaggcctccacagaacg*-3', *Foxg1-r*, 5'-*ggcaaggcatgtagcaaaag*-3'; *Gli3-f*, 5'-
691 *tgatccatctcctattcctcca*-3', *Gli3-r*, 5'-*tctggatacgtcgggctact*-3'; *Lef1-f*, 5'-*tcctgaaatccccaccttct*-3', *Lef1-*
692 *r*, 5'-*tgggataaacaggctgacct*-3'; *Lhx2-f*, 5'-*cagcttgcgcaaaagacc*-3', *Lhx2-r*, 5'-*taaaaggttgcgcctgaact*-
693 3'; *Lhx5-f*, 5'-*tgtgcaataagcagctatcca*-3'; *Lhx5-r,* 5'-*caaactgcggtccgtaca*-3'; *Otx1-f*, 5'-
694 *ccagagtccagagtccaggt*-3', *Otx1-r*, 5'-*ccgggttttcgttccatt*-3'; *Otx2-f*, 5'-*ggtatggacttgctgcatcc*-3', *Otx2-r*,
695 5'-*cgagctgtgccctagtaaatg*-3'; *Pax6-f*, 5'-*gttccctgtcctgtggactc*-3', *Pax6-r*, 5'-*accgcccttggttaaagtct*-3';
696 *Tcf4-f*, 5'-*aaatggccactgcttgatgt*-3', *Tcf4-r*, 5'-*gcaccaccggtactttgttc*-3'.
697

698 **Quantification and statistical analysis**

699 The number of specified immunofluorescent marker-positive cells was assessed by Image J
700 Cell Counter in full image fields. Three brain sections per mouse were counted for each index.
701 GraphPad Prism 7.0 (GraphPad) was used to perform statistical analysis. The data analysis
702 used one-way analysis of variance (ANOVA), Dunnett's or Tukey's post hoc tests, and
703 student's unpaired t-test. The data were expressed as the mean ± SEM. The data obtained
704 from at least three independent replicates were used for statistical analysis. $P < 0.05$ was
705 considered the significant statistical difference.
706

707 **Acknowledgements**

We thank Ms. Emerald Tang for her assistance with the manuscript. This work was supported by National Natural Science Foundation of China (31671508) and Guangdong Provincial Basic and Applied Basic Research Fund (2021A1515011299) to K.T; and in part by the National Key Basic Research and Development Program of China (2018YFA0108500, 2019YFA0801402, 2018YFA0800100, 2018YFA0108000, 2018YFA0107200, 2017YFA0102700), "Strategic Priority Research Program" of the Chinese Academy of Sciences, Grant No. (XDA16020501, XDA16020404) to N. J.

Author contributions

X.Y., W.R. designed and conducted the experiments. X.Y. and K.T. organized and wrote the manuscript. Z.W.L., S.F. and J.X.Y. assisted in conducting the experiments and analyzed the data. N.J. and K.T. conceived the project and approved the manuscript.

Competing interests

The authors declare no competing interests.

References

Abboud, S., Bar, L., Rosenfeld, M., Ring, H., & Glass, I. (1996). Left-right asymmetry of visual evoked potentials in brain-damaged patients: a mathematical model and experimental results. *Ann Biomed Eng, 24*(1), 75-86. doi:10.1007/BF02770997

Amaral, D. G. (1993). Emerging principles of intrinsic hippocampal organization. *Current Opinion in Neurobiology, 3*(2), 225-229. doi:https://doi.org/10.1016/0959-4388(93)90214-J

Anacker, C., & Hen, R. (2017). Adult hippocampal neurogenesis and cognitive flexibility - linking memory and mood. *Nat Rev Neurosci, 18*(6), 335-346. doi:10.1038/nrn.2017.45

Armentano, M., Chou, S. J., Tomassy, G. S., Leingärtner, A., O'Leary, D. D., & Studer, M. (2007). COUP-TFI regulates the balance of cortical patterning between frontal/motor and sensory areas. *Nat Neurosci, 10*(10), 1277-1286. doi:10.1038/nn1958

Baik, J. H. (2020). Stress and the dopaminergic reward system. *Exp Mol Med, 52*(12), 1879-1890. doi:10.1038/s12276-020-00532-4

Bast, T. (2007). Toward an integrative perspective on hippocampal function: from the rapid encoding of experience to adaptive behavior. *Rev Neurosci, 18*(3-4), 253-281. doi:10.1515/revneuro.2007.18.3-4.253

Basu, J., & Siegelbaum, S. A. (2015). The Corticohippocampal Circuit, Synaptic Plasticity, and Memory. *Cold Spring Harb Perspect Biol, 7*(11). doi:10.1101/cshperspect.a021733

Bertacchi, M., Romano, A. L., Loubat, A., Tran Mau-Them, F., Willems, M., Faivre, L., . . . Studer, M. (2020). NR2F1 regulates regional progenitor dynamics in the mouse neocortex and cortical gyrification in BBSOAS patients. *Embo j, 39*(13), e104163. doi:10.15252/embj.2019104163

Bliss, T. V., & Lomo, T. (1973). Long-lasting potentiation of synaptic transmission in the dentate area of the anaesthetized rabbit following stimulation of the perforant path. *J Physiol, 232*(2), 331-356. doi:10.1113/jphysiol.1973.sp010273

Bosch, D. G., Boonstra, F. N., Gonzaga-Jauregui, C., Xu, M., de Ligt, J., Jhangiani, S., . . . Schaaf, C. P. (2014). NR2F1 mutations cause optic atrophy with intellectual disability. *Am J Hum Genet, 94*(2), 303-309. doi:10.1016/j.ajhg.2014.01.002

Bryant, K. G., & Barker, J. M. (2020). Arbitration of Approach-Avoidance Conflict by Ventral Hippocampus. *Front Neurosci, 14*, 615337. doi:10.3389/fnins.2020.615337

Cenquizca, L. A., & Swanson, L. W. (2007). Spatial organization of direct hippocampal field CA1 axonal projections to the rest of the cerebral cortex. *Brain Res Rev, 56*(1), 1-26. doi:10.1016/j.brainresrev.2007.05.002

Contesse, T., Ayrault, M., Mantegazza, M., Studer, M., & Deschaux, O. (2019). Hyperactive and anxiolytic-like behaviors result from loss of COUP-TFI/Nr2f1 in the mouse cortex. *Genes Brain Behav, 18*(7), e12556. doi:10.1111/gbb.12556

Del Pino, I., Tocco, C., Magrinelli, E., Marcantoni, A., Ferraguto, C., Tomagra, G., . . . Studer, M. (2020). COUP-TFI/Nr2f1 Orchestrates Intrinsic Neuronal Activity during Development of the Somatosensory Cortex. *Cereb Cortex, 30*(11), 5667-5685. doi:10.1093/cercor/bhaa137

Eichenbaum, H. (2017). On the Integration of Space, Time, and Memory. *Neuron, 95*(5), 1007-1018. doi:10.1016/j.neuron.2017.06.036

Eichenbaum, H., & Cohen, N. J. (2014). Can we reconcile the declarative memory and spatial navigation views on hippocampal function? *Neuron, 83*(4), 764-770. doi:10.1016/j.neuron.2014.07.032

Fanselow, M. S., & Dong, H. W. (2010). Are the dorsal and ventral hippocampus functionally distinct structures? *Neuron, 65*(1), 7-19. doi:10.1016/j.neuron.2009.11.031

Feng, J., Hsu, W. H., Patterson, D., Tseng, C. S., Hsing, H. W., Zhuang, Z. H., . . . Chou, S. J. (2021). COUP-TFI specifies the medial entorhinal cortex identity and induces differential cell adhesion to determine the integrity of its boundary with neocortex. *Sci Adv, 7*(27). doi:10.1126/sciadv.abf6808

Feng, S., Xing, C., Shen, T., Qiao, Y., Wang, R., Chen, J., . . . Tang, K. (2017). Abnormal Paraventricular Nucleus of Hypothalamus and Growth Retardation Associated with Loss of Nuclear Receptor Gene COUP-TFII. *Sci Rep, 7*(1), 5282. doi:10.1038/s41598-017-05682-6

Flore, G., Di Ruberto, G., Parisot, J., Sannino, S., Russo, F., Illingworth, E. A., . . . De Leonibus, E. (2017). Gradient COUP-TFI Expression Is Required for Functional Organization of the Hippocampal Septo-Temporal Longitudinal Axis. *Cereb Cortex, 27*(2), 1629-1643. doi:10.1093/cercor/bhv336

Galceran, J., Miyashita-Lin, E. M., Devaney, E., Rubenstein, J. L., & Grosschedl, R. (2000). Hippocampus development and generation of dentate gyrus granule cells is regulated by LEF1. *Development, 127*(3), 469-482. doi:10.1242/dev.127.3.469

Gao, X., Arlotta, P., Macklis, J. D., & Chen, J. (2007). Conditional knock-out of beta-catenin in postnatal-born dentate gyrus granule neurons results in dendritic malformation. *J Neurosci, 27*(52), 14317-14325. doi:10.1523/jneurosci.3206-07.2007

Gould, E., & Cameron, H. A. (1996). Regulation of neuronal birth, migration and death in the rat dentate gyrus. *Dev Neurosci, 18*(1-2), 22-35. doi:10.1159/000111392

Hébert, J. M., & Fishell, G. (2008). The genetics of early telencephalon patterning: some assembly required. *Nat Rev Neurosci, 9*(9), 678-685. doi:10.1038/nrn2463

Herman, J. P., McKlveen, J. M., Ghosal, S., Kopp, B., Wulsin, A., Makinson, R., . . . Myers, B. (2016). Regulation of the Hypothalamic-Pituitary-Adrenocortical Stress Response. *Compr Physiol, 6*(2), 603-621. doi:10.1002/cphy.c150015

High, F. A., Bhayani, P., Wilson, J. M., Bult, C. J., Donahoe, P. K., & Longoni, M. (2016). De novo frameshift mutation in COUP-TFII (NR2F2) in human congenital diaphragmatic hernia. *Am J Med Genet A, 170*(9), 2457-2461. doi:10.1002/ajmg.a.37830

Hoover, W. B., & Vertes, R. P. (2007). Anatomical analysis of afferent projections to the medial prefrontal cortex in the rat. *Brain Struct Funct, 212*(2), 149-179. doi:10.1007/s00429-007-0150-4

Kandel, E. R., Dudai, Y., & Mayford, M. R. (2014). The molecular and systems biology of memory. *Cell, 157*(1), 163-186. doi:10.1016/j.cell.2014.03.001

Kim, B. J., Takamoto, N., Yan, J., Tsai, S. Y., & Tsai, M. J. (2009). Chicken Ovalbumin Upstream Promoter-Transcription Factor II (COUP-TFII) regulates growth and patterning of the postnatal mouse cerebellum. *Dev Biol, 326*(2), 378-391. doi:10.1016/j.ydbio.2008.11.001

Kishi, T., Tsumori, T., Ono, K., Yokota, S., Ishino, H., & Yasui, Y. (2000). Topographical organization of projections from the subiculum to the hypothalamus in the rat. *J Comp Neurol, 419*(2), 205-222. doi:10.1002/(sici)1096-9861(20000403)419:2<205::aid-cne5>3.0.co;2-0

Lee, H., GoodSmith, D., & Knierim, J. J. (2020). Parallel processing streams in the hippocampus. *Curr Opin Neurobiol, 64*, 127-134. doi:10.1016/j.conb.2020.03.004

Lee, S. M., Tole, S., Grove, E., & McMahon, A. P. (2000). A local Wnt-3a signal is required for development of the mammalian hippocampus. *Development, 127*(3), 457-467. doi:10.1242/dev.127.3.457

Leid, M., Ishmael, J. E., Avram, D., Shepherd, D., Fraulob, V., & Dolle, P. (2004). CTIP1 and CTIP2 are differentially expressed during mouse embryogenesis. *Gene Expr Patterns, 4*(6), 733-739. doi:10.1016/j.modgep.2004.03.009

Li, J., Sun, L., Peng, X. L., Yu, X. M., Qi, S. J., Lu, Z. J., . . . Shen, Q. (2021). Integrative genomic analysis of early neurogenesis reveals a temporal genetic program for differentiation and specification of preplate and Cajal-Retzius neurons. *PLoS Genet, 17*(3), e1009355. doi:10.1371/journal.pgen.1009355

Lisman, J., Buzsaki, G., Eichenbaum, H., Nadel, L., Ranganath, C., & Redish, A. D. (2017). Viewpoints: how the hippocampus contributes to memory, navigation and cognition. *Nat Neurosci, 20*(11), 1434-1447. doi:10.1038/nn.4661

Lodato, S., Tomassy, G. S., De Leonibus, E., Uzcategui, Y. G., Andolfi, G., Armentano, M., . . . Studer, M. (2011). Loss of COUP-TFI alters the balance between caudal ganglionic eminence- and medial ganglionic eminence-derived cortical interneurons and results in resistance to epilepsy. *J Neurosci, 31*(12), 4650-4662. doi:10.1523/jneurosci.6580-10.2011

Mangale, V. S., Hirokawa, K. E., Satyaki, P. R., Gokulchandran, N., Chikbire, S., Subramanian, L., . . . Monuki, E. S. (2008). Lhx2 selector activity specifies cortical identity and suppresses hippocampal organizer fate. *Science, 319*(5861), 304-309. doi:10.1126/science.1151695

Miquelajáuregui, A., Varela-Echavarría, A., Ceci, M. L., García-Moreno, F., Ricaño, I., Hoang, K., . . . Zhao, Y. (2010). LIM-homeobox gene Lhx5 is required for normal development of Cajal-Retzius cells. *J Neurosci, 30*(31), 10551-10562. doi:10.1523/jneurosci.5563-09.2010

Monuki, E. S., Porter, F. D., & Walsh, C. A. (2001). Patterning of the dorsal telencephalon and cerebral cortex by a roof plate-Lhx2 pathway. *Neuron, 32*(4), 591-604. doi:10.1016/s0896-6273(01)00504-9

Moore, S. A., & Iulianella, A. (2021). Development of the mammalian cortical hem and its derivatives: the choroid plexus, Cajal-Retzius cells and hippocampus. *Open Biol, 11*(5), 210042. doi:10.1098/rsob.210042

Moser, M. B., & Moser, E. I. (1998). Functional differentiation in the hippocampus. *Hippocampus, 8*(6), 608-619. doi:10.1002/(SICI)1098-1063(1998)8:6<608::AID-HIPO3>3.0.CO;2-7

O'Keefe, J., & Conway, D. H. (1978). Hippocampal place units in the freely moving rat: why they fire where they fire. *Exp Brain Res, 31*(4), 573-590. doi:10.1007/BF00239813

O'Keefe, J., & Dostrovsky, J. (1971). The hippocampus as a spatial map. Preliminary evidence from unit activity in the freely-moving rat. *Brain Res, 34*(1), 171-175. doi:10.1016/0006-8993(71)90358-1

O'Leary, O. F., & Cryan, J. F. (2014). A ventral view on antidepressant action: roles for adult hippocampal neurogenesis along the dorsoventral axis. *Trends Pharmacol Sci, 35*(12), 675-687. doi:10.1016/j.tips.2014.09.011

Penfield, W., & Milner, B. (1958). Memory deficit produced by bilateral lesions in the hippocampal zone. *AMA Arch Neurol Psychiatry, 79*(5), 475-497. doi:10.1001/archneurpsyc.1958.02340050003001

Pitkanen, A., Pikkarainen, M., Nurminen, N., & Ylinen, A. (2000). Reciprocal connections between the amygdala and the hippocampal formation, perirhinal cortex, and postrhinal cortex in rat. A review. *Ann N Y Acad Sci, 911*, 369-391. doi:10.1111/j.1749-6632.2000.tb06738.x

Porter, F. D., Drago, J., Xu, Y., Cheema, S. S., Wassif, C., Huang, S. P., . . . Westphal, H. (1997). Lhx2, a LIM homeobox gene, is required for eye, forebrain, and definitive erythrocyte development. *Development, 124*(15), 2935-2944. doi:10.1242/dev.124.15.2935

Roberts, A. C., Tomic, D. L., Parkinson, C. H., Roeling, T. A., Cutter, D. J., Robbins, T. W., & Everitt, B. J. (2007). Forebrain connectivity of the prefrontal cortex in the marmoset monkey (Callithrix jacchus): an anterograde and retrograde tract-tracing study. *J Comp Neurol, 502*(1), 86-112. doi:10.1002/cne.21300

Roy, A., Gonzalez-Gomez, M., Pierani, A., Meyer, G., & Tole, S. (2014). Lhx2 regulates the development of the forebrain hem system. *Cereb Cortex, 24*(5), 1361-1372. doi:10.1093/cercor/bhs421

Schuurmans, C., & Guillemot, F. (2002). Molecular mechanisms underlying cell fate specification in the developing telencephalon. *Curr Opin Neurobiol, 12*(1), 26-34. doi:10.1016/s0959-4388(02)00286-6

Scoville, W. B., & Milner, B. (1957). Loss of recent memory after bilateral hippocampal lesions. *J Neurol Neurosurg Psychiatry, 20*(1), 11-21. doi:10.1136/jnnp.20.1.11

Simeone, A., Gulisano, M., Acampora, D., Stornaiuolo, A., Rambaldi, M., & Boncinelli, E. (1992). Two vertebrate homeobox genes related to the Drosophila empty spiracles

gene are expressed in the embryonic cerebral cortex. *EMBO J, 11*(7), 2541-2550. doi:10.1002/j.1460-2075.1992.tb05319.x

Strange, B. A., Witter, M. P., Lein, E. S., & Moser, E. I. (2014). Functional organization of the hippocampal longitudinal axis. *Nat Rev Neurosci, 15*(10), 655-669. doi:10.1038/nrn3785

Sugiyama, T., Osumi, N., & Katsuyama, Y. (2014). A novel cell migratory zone in the developing hippocampal formation. *J Comp Neurol, 522*(15), 3520-3538. doi:10.1002/cne.23621

Swindell, E. C., Bailey, T. J., Loosli, F., Liu, C., Amaya-Manzanares, F., Mahon, K. A., . . . Jamrich, M. (2006). Rx-Cre, a tool for inactivation of gene expression in the developing retina. *Genesis, 44*(8), 361-363. doi:10.1002/dvg.20225

Takeda, K., Inoue, H., Tanizawa, Y., Matsuzaki, Y., Oba, J., Watanabe, Y., . . . Oka, Y. (2001). WFS1 (Wolfram syndrome 1) gene product: predominant subcellular localization to endoplasmic reticulum in cultured cells and neuronal expression in rat brain. *Hum Mol Genet, 10*(5), 477-484. doi:10.1093/hmg/10.5.477

Tang, K., Rubenstein, J. L., Tsai, S. Y., & Tsai, M. J. (2012). COUP-TFII controls amygdala patterning by regulating neuropilin expression. *Development, 139*(9), 1630-1639. doi:10.1242/dev.075564

Toda, T., Parylak, S. L., Linker, S. B., & Gage, F. H. (2019). The role of adult hippocampal neurogenesis in brain health and disease. *Mol Psychiatry, 24*(1), 67-87. doi:10.1038/s41380-018-0036-2

Tole, S., Goudreau, G., Assimacopoulos, S., & Grove, E. A. (2000). Emx2 is required for growth of the hippocampus but not for hippocampal field specification. *J Neurosci, 20*(7), 2618-2625. Retrieved from https://www.ncbi.nlm.nih.gov/pubmed/10729342

Tuncdemir, S. N., Lacefield, C. O., & Hen, R. (2019). Contributions of adult neurogenesis to dentate gyrus network activity and computations. *Behav Brain Res, 374*, 112112. doi:10.1016/j.bbr.2019.112112

Tyng, C. M., Amin, H. U., Saad, M. N. M., & Malik, A. S. (2017). The Influences of Emotion on Learning and Memory. *Front Psychol, 8*, 1454. doi:10.3389/fpsyg.2017.01454

Vorhees, C. V., & Williams, M. T. (2006). Morris water maze: procedures for assessing spatial and related forms of learning and memory. *Nat Protoc, 1*(2), 848-858. doi:10.1038/nprot.2006.116

Yang, X., Feng, S., & Tang, K. (2017). COUP-TF Genes, Human Diseases, and the Development of the Central Nervous System in Murine Models. *Curr Top Dev Biol, 125*, 275-301. doi:10.1016/bs.ctdb.2016.12.002

Yoshida, M., Suda, Y., Matsuo, I., Miyamoto, N., Takeda, N., Kuratani, S., & Aizawa, S. (1997). Emx1 and Emx2 functions in development of dorsal telencephalon. *Development, 124*(1), 101-111. doi:10.1242/dev.124.1.101

Yu, D. X., Marchetto, M. C., & Gage, F. H. (2014). How to make a hippocampal dentate gyrus granule neuron. *Development, 141*(12), 2366-2375. doi:10.1242/dev.096776

Zhang, K., Yu, F., Zhu, J., Han, S., Chen, J., Wu, X., . . . Tang, K. (2020). Imbalance of Excitatory/Inhibitory Neuron Differentiation in Neurodevelopmental Disorders with an NR2F1 Point Mutation. *Cell Rep, 31*(3), 107521. doi:10.1016/j.celrep.2020.03.085

Zhao, Y., Sheng, H. Z., Amini, R., Grinberg, A., Lee, E., Huang, S., . . . Westphal, H. (1999). Control of hippocampal morphogenesis and neuronal differentiation by the LIM homeobox gene Lhx5. *Science, 284*(5417), 1155-1158. doi:10.1126/science.284.5417.1155

Zhou, C., Qiu, Y., Pereira, F. A., Crair, M. C., Tsai, S. Y., & Tsai, M. J. (1999). The nuclear orphan receptor COUP-TFI is required for differentiation of subplate neurons and

938 guidance of thalamocortical axons. *Neuron, 24*(4), 847-859. doi:10.1016/s0896-
939 6273(00)81032-6
940 Zhou, C., Tsai, S. Y., & Tsai, M. J. (2001). COUP-TFI: an intrinsic factor for early
941 regionalization of the neocortex. *Genes Dev, 15*(16), 2054-2059.
942 doi:10.1101/gad.913601
943 Zhou, X., Liu, F., Tian, M., Xu, Z., Liang, Q., Wang, C., . . . Yang, Z. (2015). Transcription
944 factors COUP-TFI and COUP-TFII are required for the production of granule cells in
945 the mouse olfactory bulb. *Development, 142*(9), 1593-1605. doi:10.1242/dev.115279
946
947

948 **Figure legends**

949

950 **Figure 1. Duplicated CA1 and CA3 domains are generated in the ventral hippocampus**

951 **of *RXCre/*+; *CII$^{F/F}$* mutant mice.**

952 **A,** The expression of COUP-TFI (**a, d, g, j, m**) and COUP-TFII (**b, e, h, k, n**) in coronal

953 sections (**a-f**) and sagittal sections (**g-o**) of the hippocampus at postnatal month 1 (1M);

954 representative Western blots and quantitative densitometry data for the expression of COUP-

955 TFI and COUP-TFII in the dorsal and ventral hippocampus at 1M (**p-q**). **B,** In coronal

956 sections along the rostrocaudal axis (**a-f**) and sagittal sections along the lateral-medial axis

957 (**g-l**) of the hippocampus in mutant mice, compared with that in control mice (**a-c**, **g-i**), the

958 ectopic CA-like structure, indicated by the star, was observed in the ventral region in *COUP-*

959 *TFII* gene mutant (*RXCre/*+; *CII$^{F/F}$)* mice at 1M (**d-f**, **j-l**). **C,** The expression of HuB and

960 Ctip2 in the corresponding inserted area in **a-f** under a high magnification objective lens at

961 1M (**g-r**); compared with those of control mice (**a-c**, **g-i**, **m-o**), the duplicated HuB-positive

962 CA3 domain, indicated by the star, and Ctip2-positive domains, indicated by the arrowhead,

963 were specifically observed in the ventral hippocampus (**d-f, p-r**) but not in the dorsal

964 hippocampus (**d-f**, **j-l**) of *COUP-TFII* mutant mice at 1M; Ctip2 positive AHi and MePD

965 amygdaloid nuclei were barely observed in the *COUP-TFII* mutant mice, indicated by the

966 arrows, instead of the ectopic CA domains at the prospective amygdaloid regions (**e-f**, **q-r**).

967 Data are expressed as the mean ± SEM. *Student's t test*, $^{*}P<0.05$, $^{**}P<0.01$. AHi,

968 amygdalohippocampal area; AMY, amygdala nuclei; CTX, cortex; dCA1, dorsal CA1; dCA3,

969 dorsal CA3; dDG, dorsal dentate gyrus; dHPC, dorsal hippocampus; MePD, posterodorsal

970 part of the medial amygdaloid nucleus; PMCo, posteromedial cortical amygdaloid nucleus;

971 vCA1, ventral CA1; vCA3, ventral CA3; vDG, ventral dentate gyrus; vHPC, ventral

972 hippocampus. Scale bars, **Aa-c**, **Ad-f**, **Aj-o**, **Cg-r**, 100 μm; **Ag-i**, **Ba-l, Ca-f**, 200μm.

973

974 **Figure 1—figure supplement 1. The expression of *COUP-TF* genes in the early**
975 **developing hippocampus and different conditional knock mouse models.**
976 **A,** The expression of *COUP-TFI* and *COUP-TFII* genes in the forebrain at E10.5 (**a-b**) and
977 E11.5 (**c-d**). **B,** The expression of *COUP-TFI* and *COUP-TFII* genes in the developing
978 hippocampus at E12.5 (**a-c**), E14.5 (**d-f**), and P0 (**g-l**). **C,** Compared with that of control mice
979 (**a-c**), *COUP-TFII* is efficiently deleted by RXCre recombinase in the hippocampus of
980 *COUP-TFII* mutant mice at 1M (**d-f**); *COUP-TFI* is clearly deleted by RXCre recombinase
981 in the hippocampus of *COUP-TFI* mutant mice at 1M (**g-i**). Compared with that of control
982 mice (**j-l**), COUP-TFI and -TFII were efficiently deleted by RXCre recombinase at the
983 hippocampal primordium, including the MP and CH, in *COUP-TFI/-TFII* double-mutant
984 mice at E14.5 (**m-o**). **D,** Compared with that of the control mice (**a-c, g-h**), the expression of
985 *COUP-TFII* was significantly decreased in the hippocampal primordium of the homozygous
986 mutant mice at E11.5; meanwhile, the LacZ signals obviously increased in the *COUP-TFII*
987 homozygous mutant mice at E11.5 (**d-f, j-k**). Compared with that of the control mice (**i**), the
988 expression of COUP-TFI is activated in the caudal hippocampal primordium of the
989 homozygous mutant mice at E11.5 (**l**). CH, cortical hem; dHPC, dorsal hippocampus; HP,
990 hippocampal primordium; HPC, hippocampus; MP, medial pallium; vHPC, ventral
991 hippocampus. Scale bars, **Aa-d**, **Ba-f**, **Cj-o**, 200 μm; **Bg-l**, **Ca-i**, **Dg-l**, 100 μm; **Da-f**, 250 μm.
992

993 **Figure 2. The specification and differentiation of the dorsal CA1 lineage failed with the**
994 **dysplastic dorsal hippocampus in *RXCre/+*; *CI$^{F/F}$* mutant mice.**
995 **A,** In coronal sections along the rostrocaudal axis (**a-f**) and sagittal sections along the lateral-
996 medial axis (**g-l**) of the hippocampus, compared with that of control mice (**a-c**, **g-i**), the dorsal
997 hippocampus was shrunken, indicated by the star, in *COUP-TFI* gene mutant (*RXCre/+;CI$^{F/F}$)*
998 mice at 1M (**d-f**, **j-l**). **B,** The expression of HuB and Ctip2 in the corresponding inserted area

999 in **a-f** under a high magnification objective lens at 1M (**g-r**); compared with that of control
1000 mice (**a-c**, **g-i**, **m-o**), the HuB-positive CA3 domain was reduced in the dorsal hippocampus,
1001 especially the Ctip2-positive dorsal CA1, which was barely detected in *COUP-TFI* mutant
1002 mice at 1M (**d-f**, **j-l**), while their expression in the ventral hippocampus was comparable
1003 between the controls and mutants (**d-f**, **p-r**). **C,** The expression of HuB and Wfs1 in the
1004 corresponding inserted area in **a-f** under a high magnification objective lens at 1M (**g-r**); the
1005 expression of HuB and the dCA1 marker Wfs1 in the control (**a-c**, **g-i**, **m-o**) and *COUP-TFII*
1006 mutant mice (**d-f**, **j-l**, **p-r**) at 1M. Wfs1-positive dorsal CA1 could not be detected in *COUP-*
1007 *TFI* mutant mice at 1M, as indicated by the arrowhead. dHPC, dorsal hippocampus; HPC,
1008 hippocampus; vHPC, ventral hippocampus. Scale bars, **Aa-l**, **Ba-f**, **Ca-f,** 200 μm; **Bg-r**, **Cg-r,**
1009 100 μm.
1010
1011 **Figure 2—figure supplement 1. Defects in *Emx1Cre/*+; *COUP-TFI$^{F/F}$* mutant mice.**
1012 **A,** Immunofluorescence staining data showed that compared with those of control mice (**a, c,**
1013 **e, g**), the proportions of either the Wfs1- or Ctip2-positive dorsal CA1 domain were reduced
1014 in *Emx1Cre/*+; *COUP-TFI$^{F/F}$* mutant mice at 3M (**b, d, f, h**). **B,** Golgi staining showed that
1015 compared with those of controls, the numbers of branch points and secondary dendrites of
1016 both apical and basal dendrites were significantly reduced in the dorsal hippocampal CA1
1017 pyramidal neurons of *Emx1Cre/*+; *COUP-TFI$^{F/F}$* mutant mice (**a-c**). **C,** The Morris water
1018 maze behavior test showed that compared with that of controls, spatial learning and memory
1019 were significantly damaged in *Emx1Cre/*+; *COUP-TFI$^{F/F}$* mutant mice. Data are expressed as
1020 the mean ± SEM. *Student's t test*, $^{*}P<0.05$, $^{**}P<0.01$, $^{***}P<0.001$. Scale bars, **Aa-h,** 100 μm;
1021 **Ba-b,** 50 μm.
1022

1023 **Figure 3. Defects in the hippocampus in *RXCre/+*; *CI$^{F/F}$*; *CII$^{F/F}$* double-gene mutant**
1024 **mice.**
1025 **A,** In coronal sections along the rostrocaudal axis, compared with control mice (**a-d**), the
1026 hippocampus was atrophic in *RXCre/+*; *CI$^{F/F}$; CII$^{F/F}$* double mutant mice, indicated by the
1027 star, and an ectopic unknown nucleus was observed in the caudal plates, indicated by the
1028 arrowhead (**e-h**). **B,** Compared with that of control mice (**a-c**, **g-i**), the expression of HuB,
1029 Ctip2, and Prox1 was decreased in the hippocampus of *COUP-TFI/-TFII* double-gene mutant
1030 mice at 3 weeks postnatal (3W) (**d-f**, **j-l**). **C,** Compared with that of control mice (**a-c**, **g-i**),
1031 the expression of HuB could not be detected in the presumptive CA3 domain, and the
1032 expression of Ctip2 or Prox1 could not be detected in the presumptive DG domain of the
1033 prospective ventral hippocampus of *RXCre/+*; *CI$^{F/F}$*; *CII$^{F/F}$* double mutant mice. Scale bars,
1034 **Aa-h**, 200 μm; **Ba-l**, **Ca-l,** 100 μm.
1035
1036 **Figure 3—figure supplement 1. Adult neurogenesis was abnormal in the hippocampi of**
1037 ***COUP-TFI/-TFII* double-gene mutant mice.**
1038 **A,** The expression of GFAP and Nestin, markers of NSCs, in the SGZ of the vDG in control
1039 and *COUP-TFII* mutant mice at 1M (**a-h**), in the SGZ of the dDG in control and *COUP-TFI*
1040 mutant mice at 1M (**i-p**) and in the SGZ of the DG in control and *COUP-TFI/-TFII* double-
1041 gene mutant mice at 3W (**q-x**). **B**, The expression of Dcx, a marker of newborn neurons, in
1042 the SGZ of the vDG in control and *COUP-TFII* mutant mice at 1M (**a-d**), in the SGZ of the
1043 dDG in control and *COUP-TFI* mutant mice at 1M (**e-h**) and in the SGZ of the DG in control
1044 and *COUP-TFI/-TFII* double-gene mutant mice at 3W (**i-l**). **C,** Quantitative analysis of
1045 GFAP/Nestin-positive cells (**a**) and Dcx-positive cells (**b**) in the SGZ of the DG in control
1046 and *COUP-TFI/-TFII* double-gene mutant mice at 3W. The numbers of GFAP and Nestin
1047 double-positive NSCs and Dcx-positive newborn neurons were significantly reduced in

1048 double-mutant mice. Data are expressed as the mean ± SEM. *Student's t test*, $^{**}P<0.01$,
1049 $^{***}P<0.001$. dDG, dorsal DG; NSC, neural stem cell; SGZ, subgranular zone; vDG, ventral
1050 DG. Scale bars, **Aa-x**, 50 μm; **Ba-l**, 100 μm.
1051
1052 **Figure 4. The impairment of hippocampal trisynaptic connectivity in *COUP-TFII***
1053 **single-gene, *COUP-TFI* single-gene, and *COUP-TFI/-TFII* double-gene mutant mice.**
1054 **A,** The expression of Calretinin, Calbindin, and SMI312 in the ventral hippocampus of the
1055 control (**a-b**, **e-f**, **i-j**) and *COUP-TFII* single-gene mutant mice (**c-d**, **g-h**, **k-l**). **B,** The
1056 expression of Calretinin, Calbindin, and SMI312 in the dorsal hippocampus of the control (**a-**
1057 **b**, **e-f**, **i-j**) and *COUP-TFI* single-gene mutant mice (**c-d**, **g-h**, **k-l**). **C,** The expression of
1058 Calretinin, Calbindin, and SMI312 in the hippocampus of the control (**a-b**, **e-f**, **i-j**) and
1059 *COUP-TFI*/*-TFII* double-gene mutant mice (**c-d**, **g-h**, **k-l**). dHPC, dorsal hippocampus; HPC,
1060 hippocampus; vHPC, ventral hippocampus. Scale bars, **Aa-l**, **Ba-l**, **Ca-l**, 100 μm.
1061
1062 **Figure 5. *COUP-TF* genes regulate the expression of key genes associated with early**
1063 **hippocampal development.**
1064 **A,** The expression profiles of genes involved in hippocampal development in control and the
1065 double mutant mice at E11.5. **B,** Compared with that of control mice (**a-b**, **a'-b', a''-b'', i-j,**
1066 **i'-j', q-r, q'-r'**), the expression of Lhx5 was reduced in double-mutant mice at E11.5 (**c-d**,
1067 **c'-d', c''-d''**), E13.5 (**k-l**, **k'-l'**) and E14.5 (**s-t**, **s'-t'**); the expression of Lhx2 was
1068 comparable between the control and double-mutant mice at E11.5 (**e-h**, **e'-h'**); and compared
1069 with that of control mice (**m-n**, **m'-n'**, **u-v**, **u'-v'**), the expression of Lhx2 was increased in
1070 double-mutant mice at E13.5 (**o-p**, **o'-p'**) and E14.5 (**w-x**, **w'-x'**). **C,** Compared with that of
1071 control mice (**a-b**, **a'-b'**), the expression of Sox2 was normal in double-mutant mice at E14.5
1072 (**c-d**, **c'-d'**); compared with that of control mice (**e-f**, **e'-f'**), the expression of Tbr2 was

1073 decreased in *COUP-TF* mutant mice at E14.5 (**g-h**, **g'-h'**); compared with that of control
1074 mice (**i-j**, **i'-j'**), the expression of NeuroD1 was reduced in double-mutant mice at E14.5 (**k-l**,
1075 **k'-l'**). **D,** Quantitative analysis of Tbr2-positive cells and NeuroD1-positive cells in **Ce'-h'**
1076 and **Ci'-l'**. **E,** In the hippocampal primordium of the early embryo, *COUP-TFI* is expressed
1077 dorsally in the MP, and *COUP-TFII* is expressed ventrally in the CH. In the mature
1078 hippocampus, the expression of *COUP-TFI* is higher in the dorsal hippocampus, which is
1079 related to spatial learning and memory, and the expression of *COUP-TFII* is mainly in the
1080 ventral hippocampus, which is associated with emotion and anxiety (**a**). Our findings support
1081 a novel molecular mechanism by which *COUP-TFI* and *COUP-TFII* may cooperate to ensure
1082 the appropriate morphogenesis and functions of the hippocampus by modulating the *Lhx5-*
1083 *Lhx2* axis (**b**). Data are expressed as the mean ± SEM. *Student's t test*, $^{**}P<0.01$. CH, cortical
1084 hem; ChP, choroid plexus; DP, dorsal pallium; HP, hippocampal primordium; MP, medial
1085 pallium. Scale bars, **Ba-x, Ca-l**, 200 μm.

1086

1087 **Figure 5—figure supplement 1. *COUP-TFI* and *-TFII* genes coordinate to control**
1088 **distinct characteristics of the hippocampus.**

1089 Roles of *COUP-TFI* and *COUP-TFII* genes in the development and function of the
1090 hippocampus and the association with neurological diseases. *COUP-TFI* is required for the
1091 morphogenesis of the dorsal hippocampus and the specification of dorsal CA1 pyramidal
1092 neuron lineage, which are associated with neurodevelopmental disorders, including ID and
1093 ASD. *COUP-TFII* is required to prevent the duplication of the CA1 and CA3 lineages of the
1094 ventral hippocampus, which may be related to psychiatric diseases such as depression,
1095 anxiety, or schizophrenia. The *COUP-TFI* and *COUP-TFII* genes are novel intrinsic
1096 regulatory genes, which cooperate with each other to ensure the early morphogenesis of the
1097 hippocampus.

Figure 1, Yang et al.

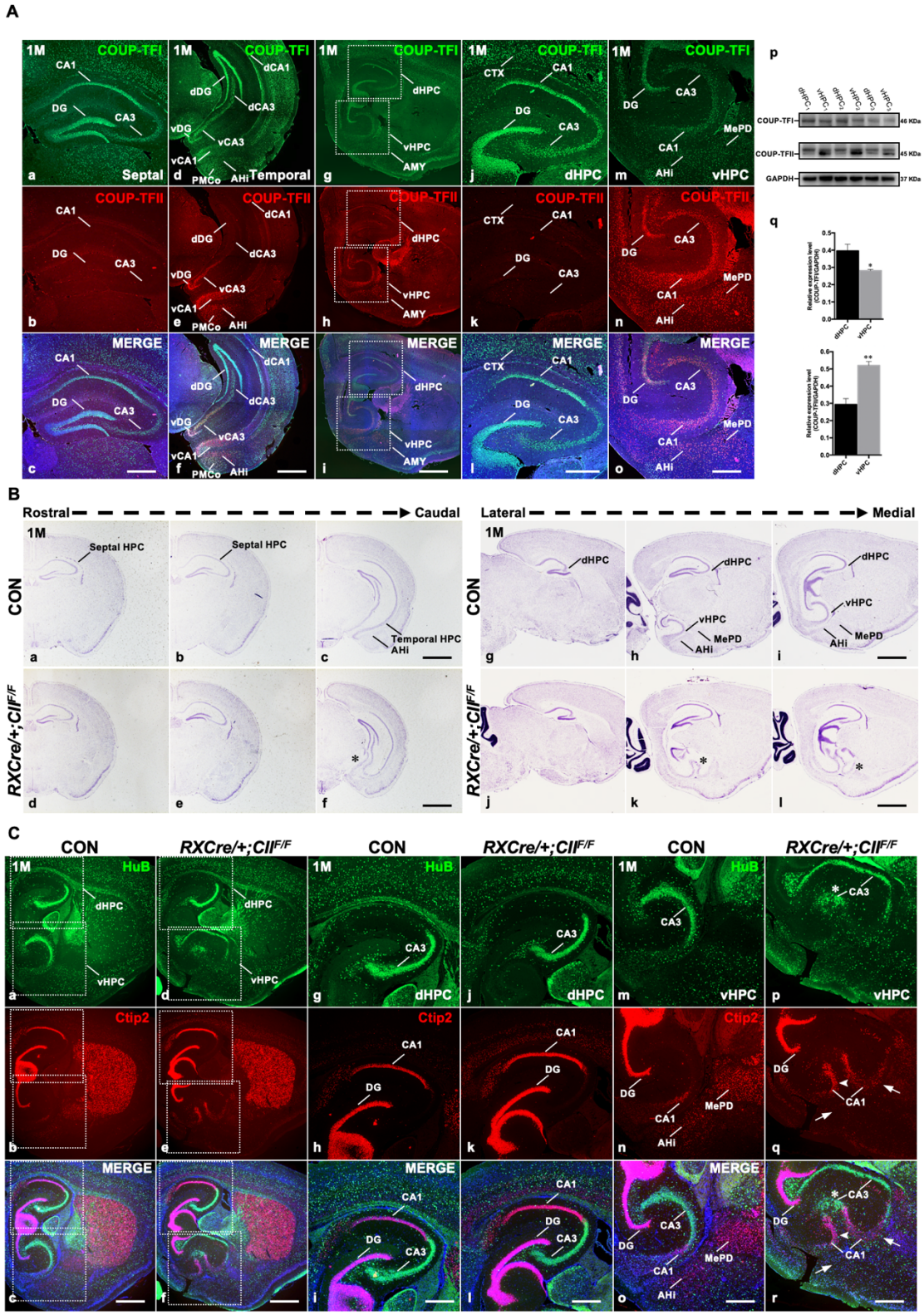

Figure 1—figure supplement 1, Yang et al.

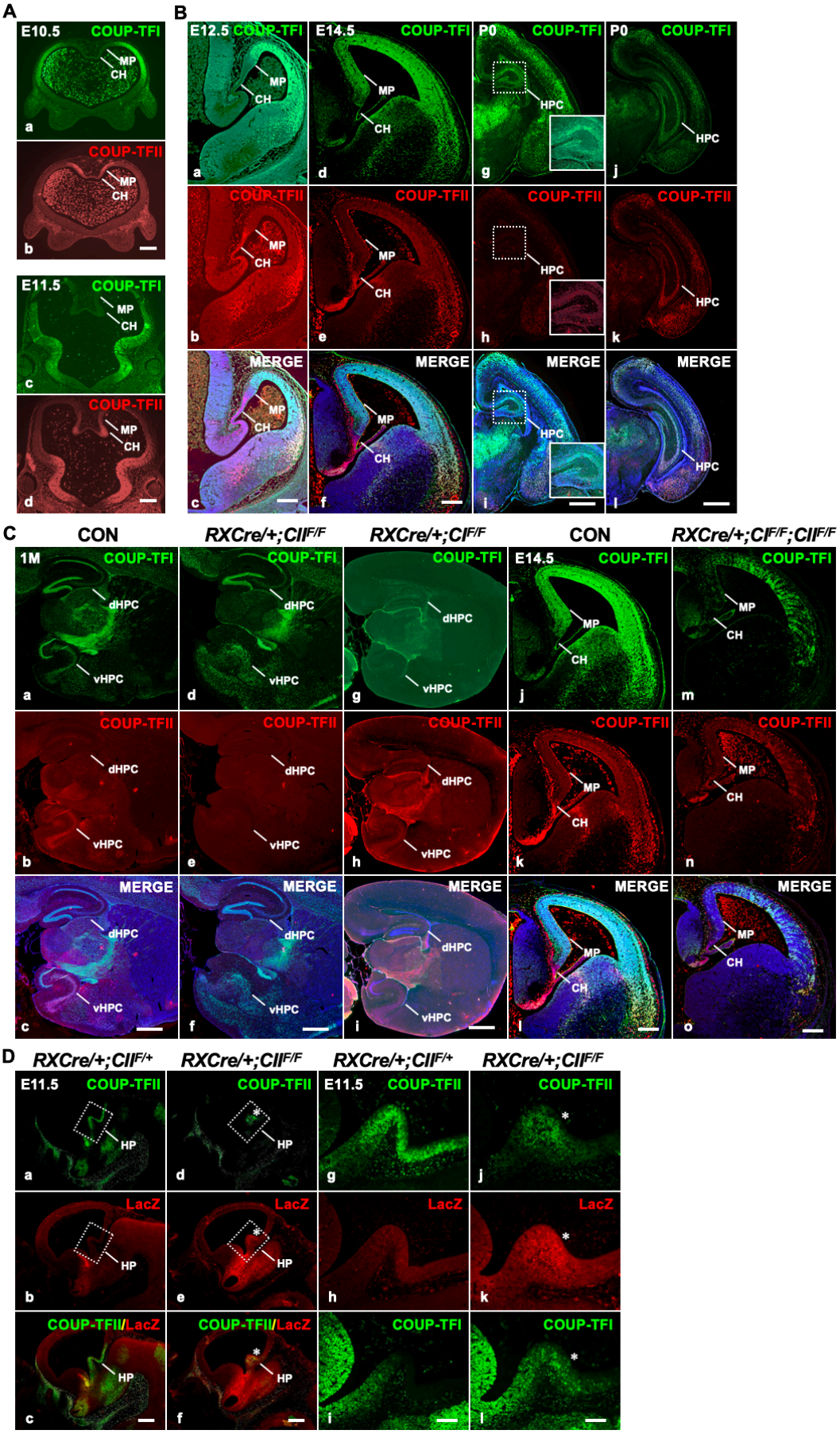

Figure 2, Yang et al.

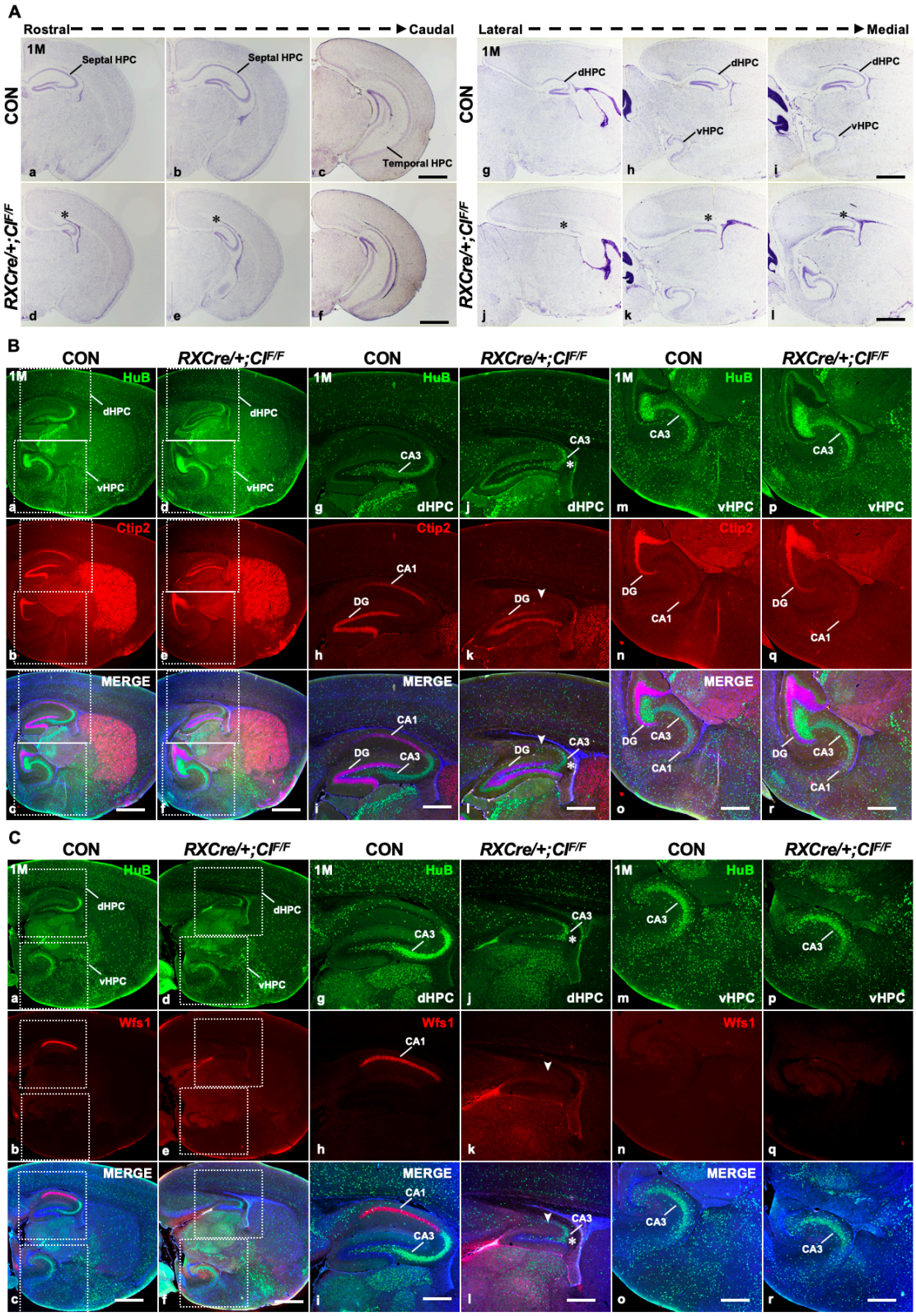

Figure 2—figure supplement 1, Yang et al.

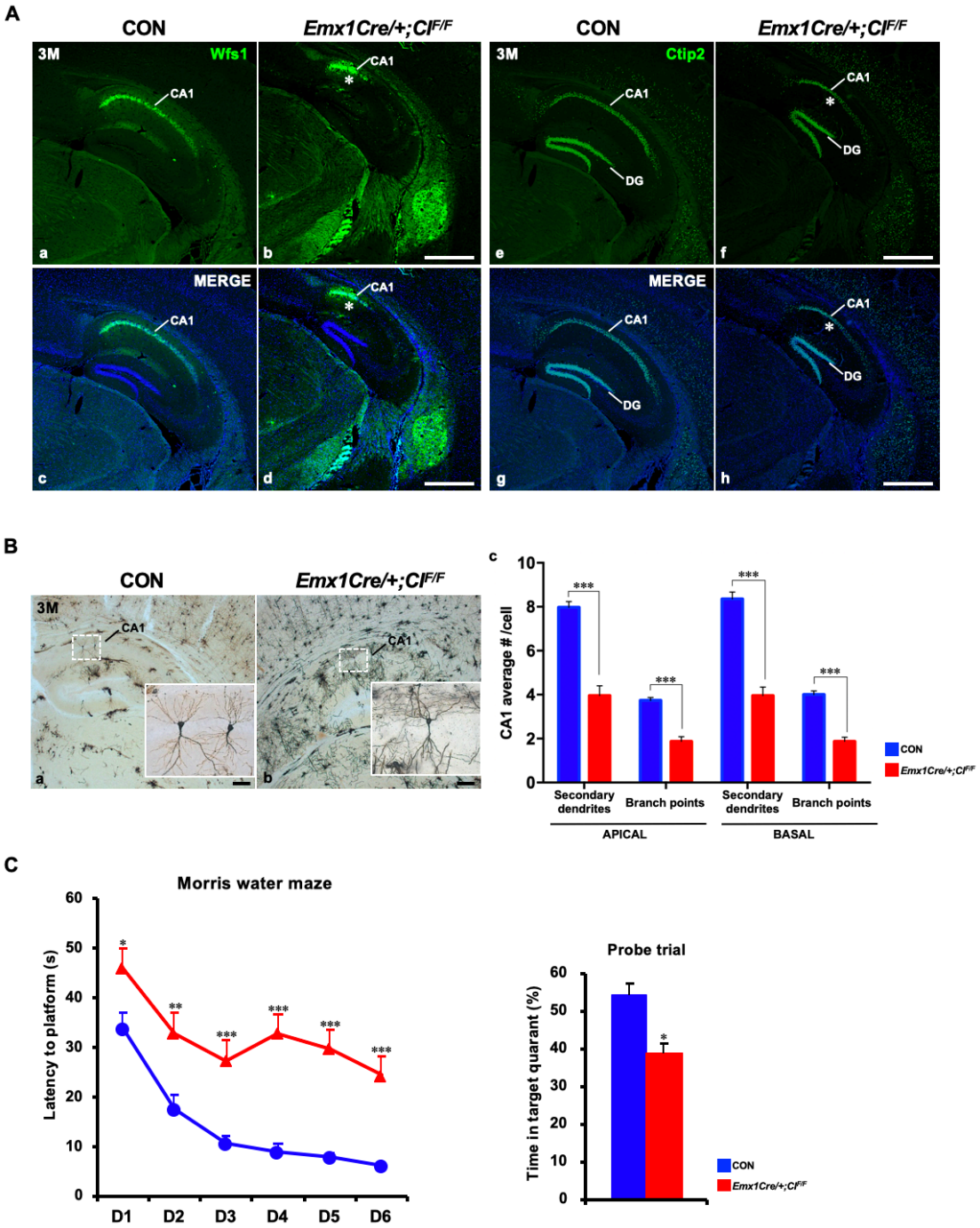

Figure 3, Yang et al.

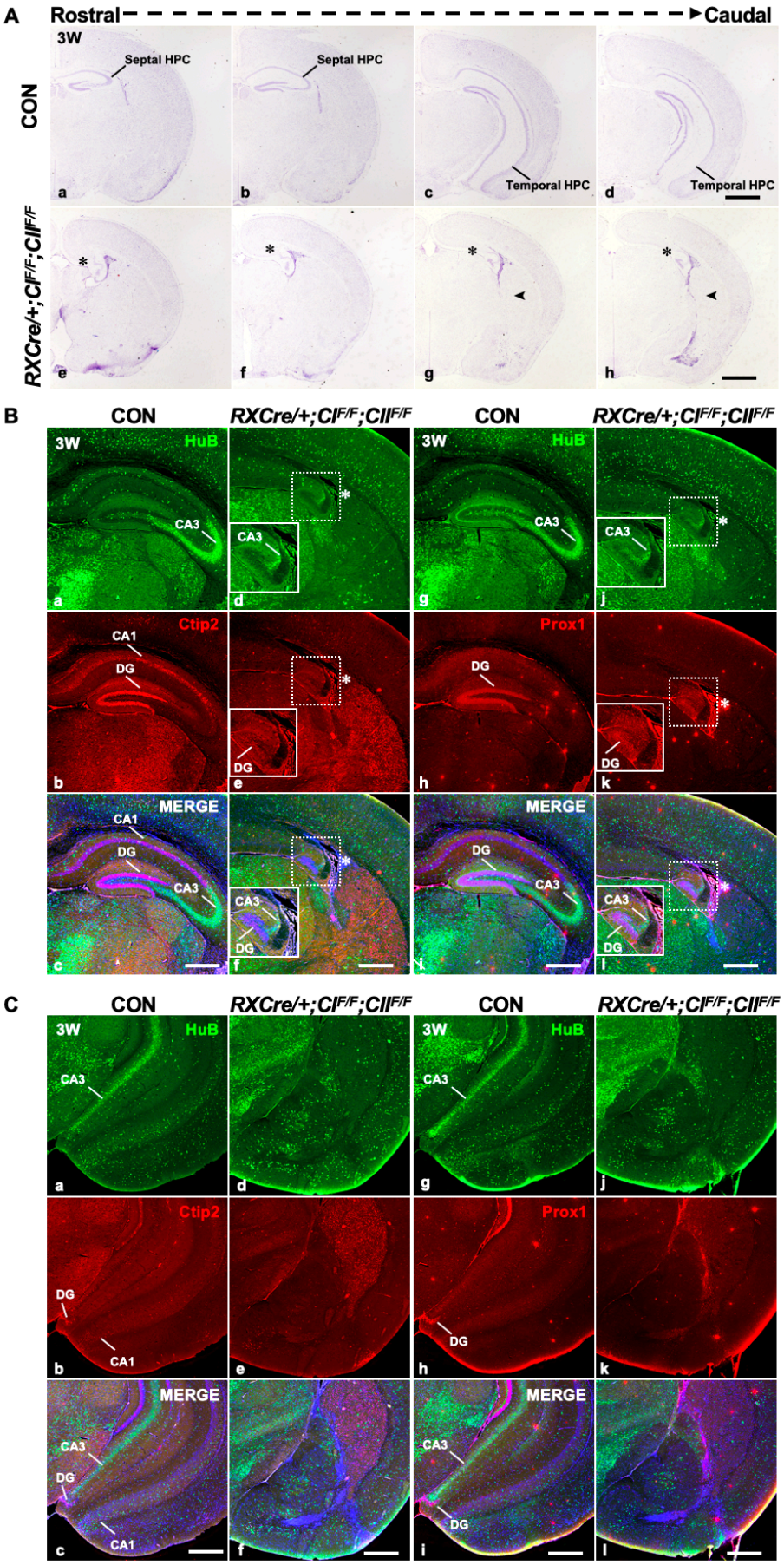

Figure 3—figure supplement 1, Yang et al.

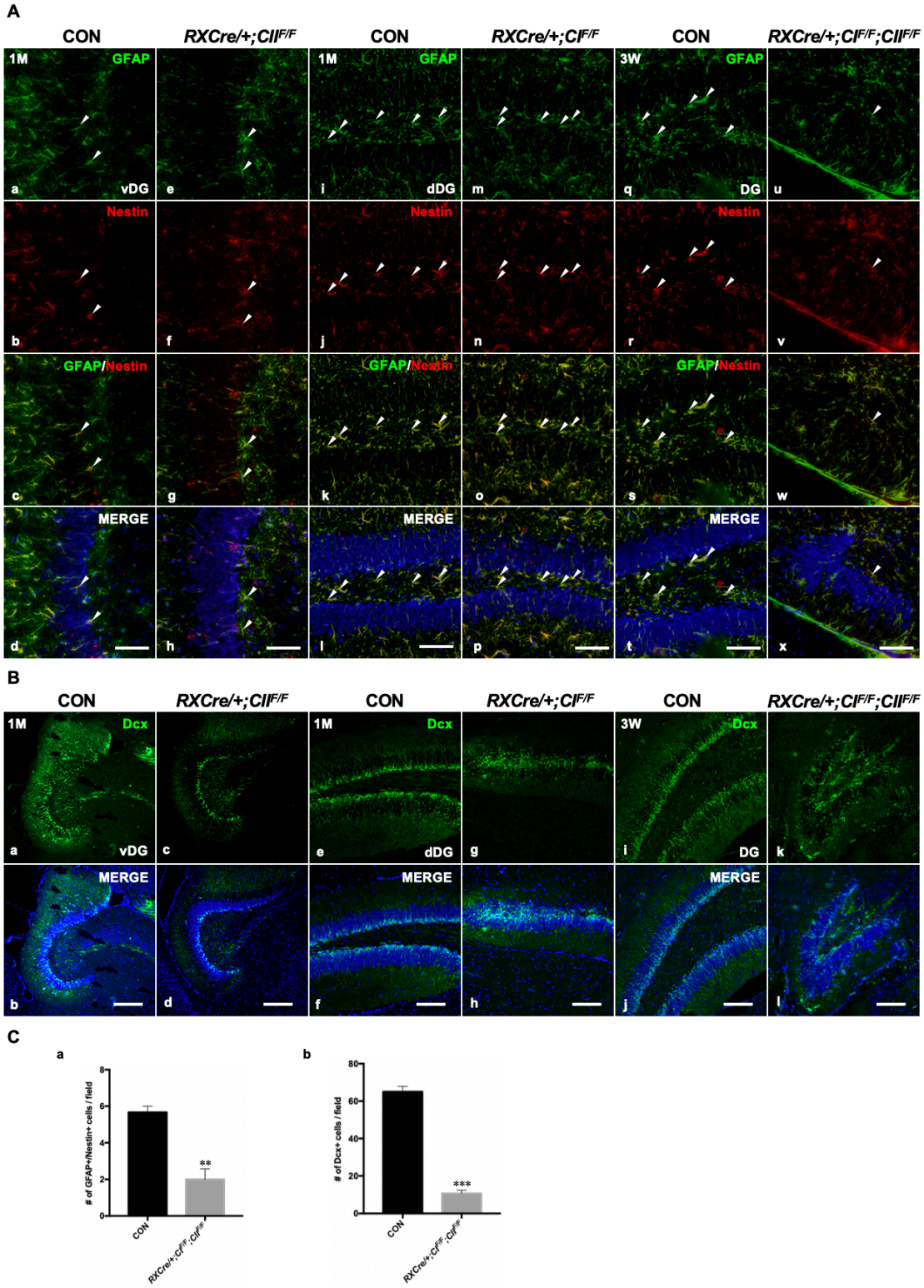

Figure 4, Yang et al.

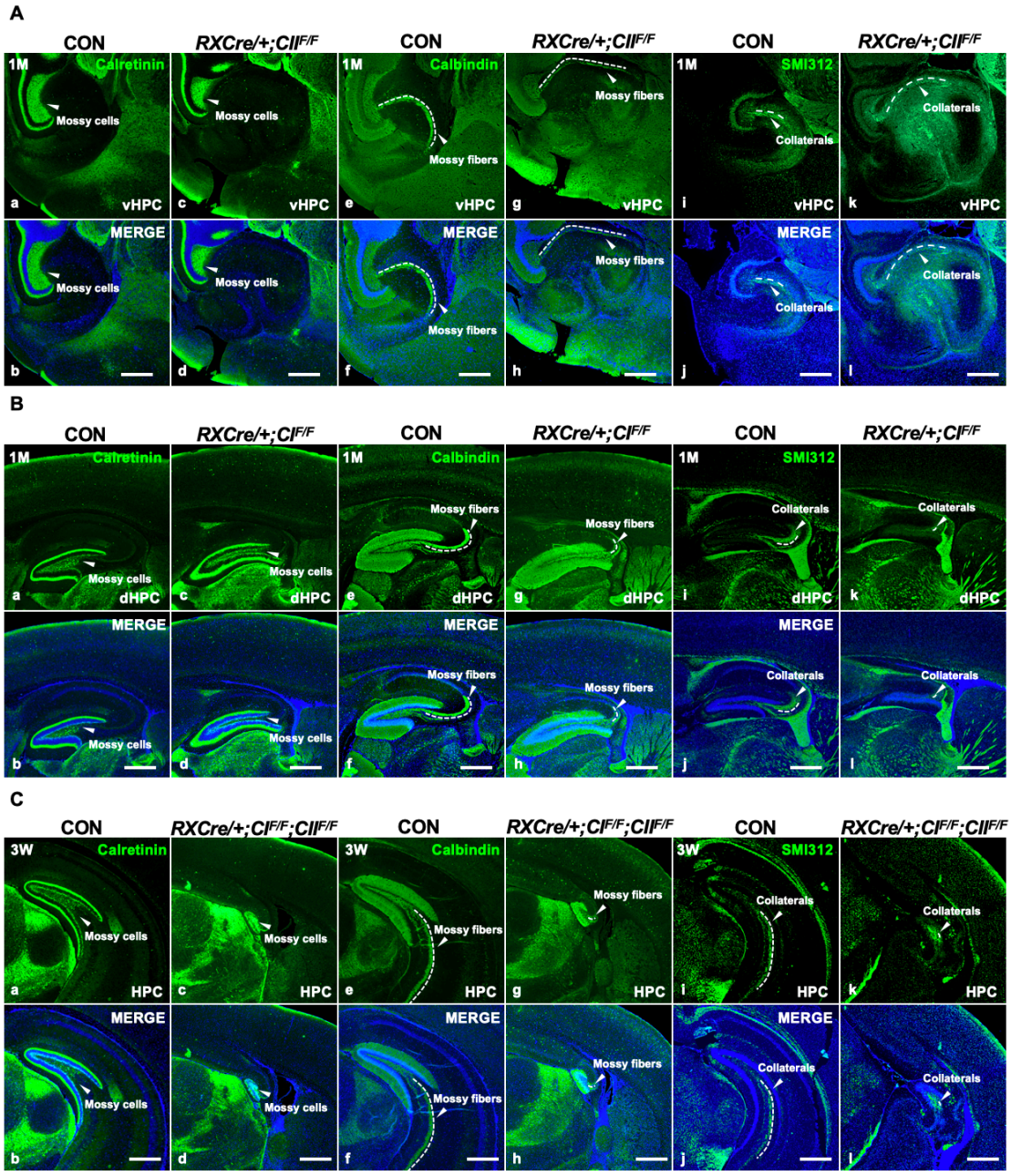

Figure 5, Yang et al.

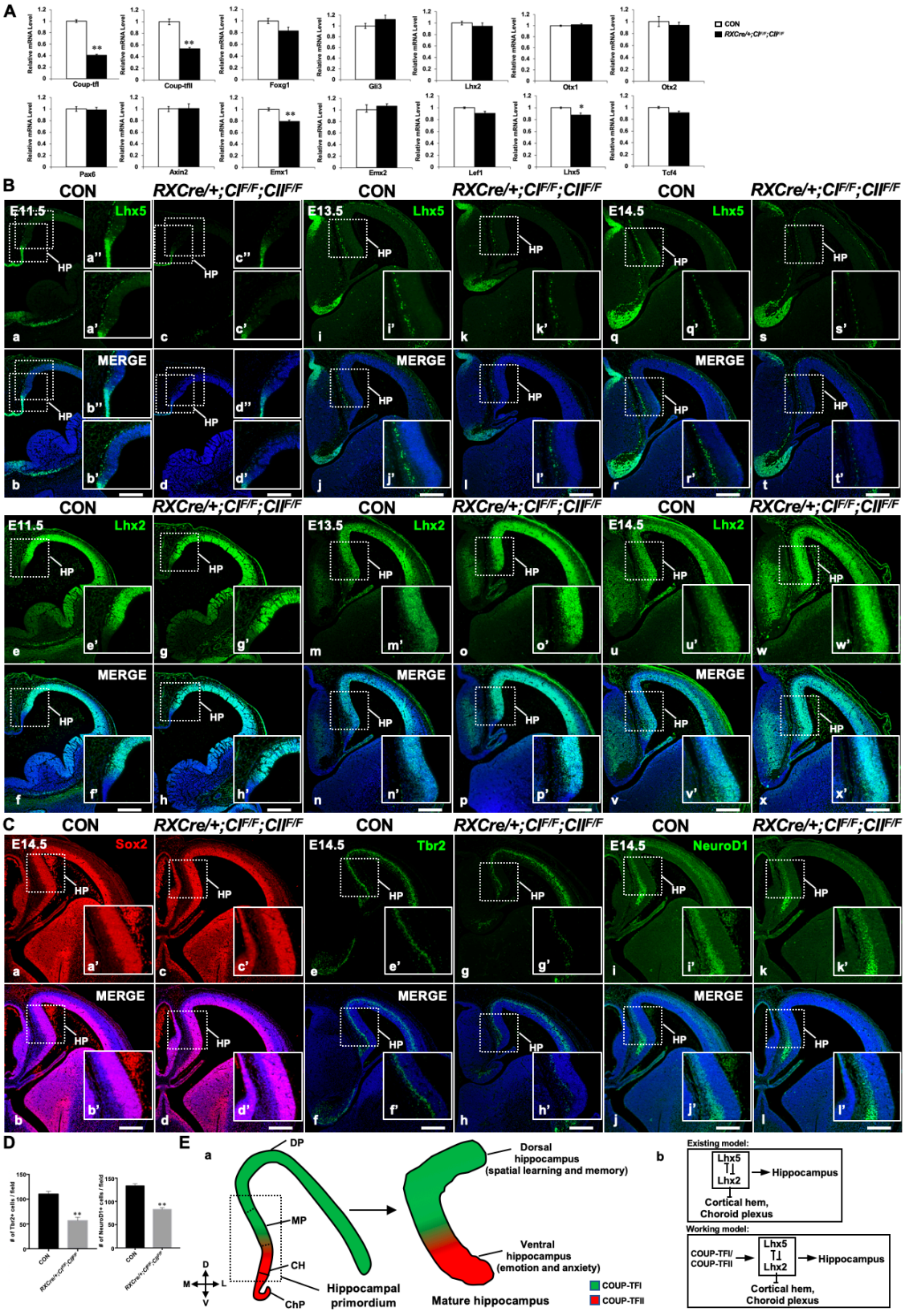
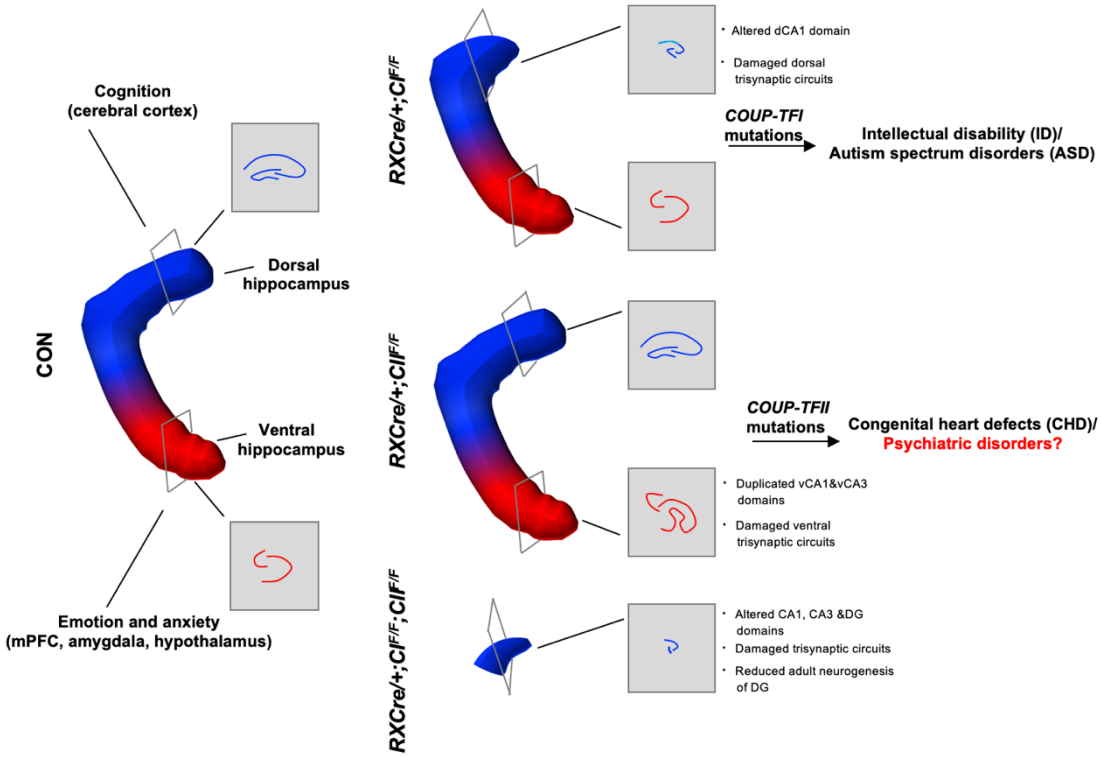
Figure 5—figure supplement 1, Yang et al.